

Developmental Neurotoxicity Testing of Nano-particle in  
Neurosphere Assays Using Human Neuronal Progenitor Cells

July 2017

Yang ZENG

Developmental Neurotoxicity Testing of Nano-particle in  
Neurosphere Assays Using Human Neuronal Progenitor Cells.

A Dissertation Submitted to  
the Graduate School of Life and Environmental Sciences,  
the University of Tsukuba  
in Partial Fulfillment of the Requirements  
for the Degree of Doctor of Philosophy in Biotechnology  
(Doctoral Program in Bioindustrial Sciences)

Yang ZENG

## **Abstract**

The contamination of neurotoxicants in food and the environment has been implicated in increases in neuronal disease in advanced countries. Moreover, the practical application of engineered nanomaterials or nanoparticles has been promoted in medical devices or industrial uses. However, the neurotoxicity of nanomaterials in human body remains unclear. Especially, the developing nervous system is highly vulnerable to the adverse effects of chemical agents. Therefore, to assess the developmental neurotoxicity (DNT) of engineered nanomaterials, a three-dimensional neurosphere culture system was developed based on human neural progenitor cells (hNPCs).

In chapter 1, the background of this research was described. PAMAM dendrimer nanoparticles, developmental neurotoxicity, human neural progenitor cells and three-dimensional neurosphere culture system were introduced. The research objective was proposed.

In chapter 2, to assess DNT of chemicals and nanomaterials, a stable and efficient neurospheres culture system was established using human neuronal progenitor cells (hNPCs). To optimization of neurosphere assays, spheres were cultured of hNPCs on a Laminin 511 (LM511) matrix to elucidate whether LM511-enriched basement membrane promotes neurite outgrowth from hNPCs. Cells cultured on the LM511 matrix exhibited increased neurite lengths compared with those cultured on Laminin 111 (LM111). The results showed that LM511 is an

appropriate and stable matrix for neurosphere culturing, and that integration of lamina-dense structure provides an ideal surface for neurite outgrowth. It suggests that these extracellular microenvironments provide binding sites for neural progenitor cells, activating intracellular signaling pathways and promoting sphere formation and neurite differentiation. Further, chemicals like benzo[a]pyrene and 5-Azacytidine were applied to our established system. Both chemicals significantly inhibited cell migration and induced apoptosis.

In chapter 3, DNT of PAMAM dendrimer nanoparticles was assessed using established culture system and was investigated by morphologic approach. Biodistribution was investigated using fluorescence-labeled nanomaterials, and observed by confocal microscopy. Neurospheres were made as three-dimensional structures consisting of neural progenitor cells on free-floating in a well. Proliferation, migration, differentiation, and apoptosis, which are basal process of brain development, are able to evaluate chemical activity in the 3-D assay. Gene expression was evaluated using microarray analysis followed by pathway and network analysis. Results showed a reduced number of MAP2-positive cells but not neurite length/cells after PAMAM-HN<sub>2</sub> exposure, indicating an inhibitory effect on neuronal migration but not differentiation. PAMAM-SC (sodium carboxylate) did not affect neurospheres at any test concentrations, suggested that natural charged PAMAM-SC will be a candidate of drug carrier. Network and pathway analysis showed Early growth response gene 1 (*EGRI*), Insulin-like growth factor-binding protein 3 (*IGFBP3*),

Tissue factor pathway inhibitor (*TFPI2*), and Adrenomedullin (*ADM*) were key genes connected with PAMAM-NH<sub>2</sub> dendrimers exposure. The expressions of these genes were then confirmed with RT-PCR.

Collectively, the neurosphere culture system can efficiently and stably be established and is a good tool for investigations of the roles of neurotoxins or therapeutic agents in neuronal disease. Neurotoxicity testing showed that the exposure of neurospheres to PAMAM-HN<sub>2</sub> during fetal development affects cell migration through *Egr1*, *IGFBP3*, *TFPI2*, and *ADM* regulated pathways. PAMAM-SC did not affect neurospheres at any test concentrations, suggested that natural charged PAMAM-SC will be a candidate of drug carrier.

**Keywords:** neurosphere assays, human neural progenitor cells, neural development, fetal toxicology, PAMAM dendrimer nanopartic

# Contents

Abstract .....	i
Contents.....	iv
List of figures .....	vi
List of tables .....	viii
Abbreviations .....	ix
Chapter 1 Introduction.....	1
1.1 Dendrimer nanoparticles .....	1
1.2 Polyamidoamine (PAMAM) dendrimers .....	1
1.3 Developmental neurotoxicity testing .....	3
1.4 Three-dimensional neurosphere .....	4
1.5 Human neural progenitor cells .....	6
1.6 Innovative point and structure in this thesis .....	7
Chapter 2 Optimization of neurosphere assays for developmental neurotoxicity testing .....	11
2.1 Introduction .....	11
2.2 Materials and methods.....	13
2.2.1 Chemicals .....	13
2.2.2 hNPC sphere formation and neural cell differentiation on the extracellular matrix .....	13
2.2.3 Immunohistochemistry staining .....	14
2.2.4 Image analysis for neurite outgrowth .....	15
2.3 Results .....	16
2.3.1 Neurosphere formation and differentiation.....	16
2.3.2 Benzo[a]pyrene and 5-Azacytidine exposure .....	17
2.4 Discussion and summary .....	17
Chapter 3 Effects of PAMAM dendrimers nanoparticles on neurosphere .....	29
3.1 Introduction .....	29
3.2 Materials and methods.....	31
3.2.1 Dendrimers and test chemicals .....	31
3.2.2 Reagents for cell-based assays.....	31
3.2.3 Neurosphere formation and Incorporation of Alexa-labeled PAMAM .....	32
3.2.4 Immunofluorescence and morphological analysis .....	32
3.2.5 Microarray and bioinformatics analysis .....	34
3.2.6 Quantitative gene expression analysis .....	35
3.2.7 Statistical analysis.....	36
3.3 Results .....	36
3.3.1 Neurosphere assay for assessing test chemicals .....	36
3.3.2 Incorporation of PAMAM dendrimers in neurospheres .....	37
3.3.3 Effect of PAMAM dendrimers on proliferation and migration of neurospheres... ..	38
3.3.4 Effect of PAMAM dendrimers on neuronal differentiation of neurospheres .....	38
3.3.5 Gene expression profiling in PAMAM dendrimer-exposed spheres by microarray analyses and RT-PCR .....	39

3.4 Discussion and Summary .....	40
Chapter 4 Conclusions and future research .....	60
4.1 Conclusions in chapter 2 .....	60
4.2 Conclusions in chapter 3 .....	60
4.3 Conclusions of this thesis .....	61
4.4 Future work .....	62
Acknowledgments .....	63
References .....	64

## List of figures

<b>Fig. 1-1</b> Structure of PAMAM dendrimer generation 1 and generation 4.....	9
<b>Fig. 1-2</b> Human neural progenitor cells (hNPCs) can differentiate into different types of neuronal cells. ....	10
<b>Fig. 2-1</b> Procedures of neurosphere culturing.....	20
<b>Fig. 2-2</b> Culture schedules (A) and photographs (B) of sphere formation, differentiation and migration.. .	21
<b>Fig. 2-3</b> Quantitative analysis of expanding corona area neurospheres (R2-R1), examined by fluorescence microscopy. ....	22
<b>Fig. 2-4</b> Immunofluorescence of MAP2-positive hNPCs at expanding corona on LM511-coated plates, LM511+LM111-coated plates and PLO/LM511+LM111-coated plates.....	23
<b>Fig. 2-5</b> Typical outgrowth of neurosphere..	24
<b>Fig. 2-6</b> Schematic of chemical exposure of neurospheres (A). Typical outgrowth of neurosphere exposed to BaP, four parallel spheres were tested for each concentration (B)..	25
<b>Fig. 2-7</b> Quantitative analysis of exposed to BaP at concentrations of $10^{-7}$ - $10^{-5}$ g/ml for corona area (A). Quantitative analysis for neurite length / MAP2-positive cell and nuclei member counting (B).....	26
<b>Fig. 2-8</b> Typical outgrowth of neurosphere exposed to 5AZ.....	27
<b>Fig. 2-9</b> Quantitative analysis of exposed to 5AZ at concentrations of $3 \times 10^{-8}$ -	

3x10 <sup>-7</sup> g/ml.....	28
<b>Fig. 3-1</b> Experimental time schedules of PAMAM exposure, proliferation and differentiation (A). Morphological photographs for proliferation and differentiation of hNPCs in the neurosphere assay (B–F). .....	46
<b>Fig. 3-2</b> Distribution images of PAMAM-NH <sub>2</sub> dendrimers using a confocal laser microscope. ....	47
<b>Fig. 3-3</b> Effects of PAMAM dendrimer on migration and proliferation of neurosphere. ....	48
<b>Fig. 3-4</b> Quantified data on the effects on proliferation and migration of PAMAM-NH <sub>2</sub> .....	49
<b>Fig. 3-5</b> Effects of PAMAM dendrimer on migration and differentiation of neurosphere. ....	50
<b>Fig. 3-6</b> Quantified data on the effects on migration of PAMAM-NH <sub>2</sub> .....	51
<b>Fig. 3-7</b> Photographs and quantified data of neurite length and nuclei number after PAMAM-NH <sub>2</sub> treatment. ....	52
<b>Fig. 3-8</b> Neurite lengths (A) and nuclei number (B) were measured. ....	53
<b>Fig. 3-9</b> Network analysis of genes with more than 1.5-fold changes selected from microarray analysis. ....	54
<b>Fig. 3-10</b> Expression of selected genes was analyzed by RT-PCR. ....	57

## List of tables

**Table 3-1.** Functional annotation pathway listed by pathway analysis. ....57

**Table 3-2.** Pathway analyses after PAMAM dendrimer exposure.. ....57

## Abbreviations

ANOVA	analysis of variance
BSA	bovine serum albumin
BAP	benzo[a]pyrene
BM	basement membrane
DNT	developmental neurotoxicity
ECM	extracellular matrix
EdU	5-ethynil-2'-deoxyuridine
HNPCs	human neural progenitor cells
LM511	laminin 511
LM111	laminin 111
MAP2	mouse anti-microtubule-associated protein 2
NDM	neural differentiation medium
NPS	neuronal progenitor sphere
NEM	neural expansion medium
NLP	natural language processing
PBS	phosphate buffered saline
PLO	poly-L-ornithine
PAMAM	polyamidoamine
PAMAM-NH <sub>2</sub>	amino-terminated PAMAM
PAMAM-SC	sodium carboxylate-terminated PAMAM
RT-PCR	reverse transcription polymerase chain reaction
SEA	single experiment analysis
5AZ	5-Azacytidine

# Chapter 1 Introduction

## 1.1 Dendrimer nanoparticles

Dendrimers are at the forefront of research in nanotechnology because of several interesting properties of macromolecular systems, including their precise architecture, high uniformity and purity, high loading capacity, and high shear resistance <sup>[1]</sup>. They have shown a great deal of versatility with applications in various areas such as drug delivery, medical therapy, electrochemistry, metal recovery, and sensors <sup>[2, 3]</sup>.

Dendrimers are nano sized particles composed of highly branched polymers. Their particle size and surface functional groups can be flexibly controlled when synthesized, which is advantageous for applications in electronic, cosmetics, automotive, and medical fields. Moreover, dendrimers have a radial structure with a large internal free volume, making them suitable as drug carriers <sup>[4, 5]</sup> and as transfection agents for DNA and oligonucleotides <sup>[6, 7]</sup>.

## 1.2 Polyamidoamine (PAMAM) dendrimers

Polyamidoamine (PAMAM) dendrimers are a common type of dendrimers that have a radial structure consisting of a 2-carbon ethylenediamine core and functional groups on their surfaces. These functionalized surface groups can be easily changed, enhancing their wide use for biological applications such as drug <sup>[8]</sup> or gene delivery <sup>[9, 10]</sup>. PAMAM can be synthesized from generation 0 (G0) to G10, the structure of G1

and G4 was showed in Fig 1-1. The probability of human exposure to PAMAM dendrimers during infancy may increase because of their potential usage. Moreover, developing nervous system is highly vulnerable to the adverse effects of chemical agents. In these cases, the assessment of the developmental neurotoxicity of PAMAM dendrimers is very important.

Polyamidoamine (PAMAM) dendrimers are a typical type of dendrimers that have a radial structure consisting of a multi-carbon ethylenediamine core and functional groups on their surfaces. The probability of human exposure to PAMAM dendrimers has arisen due to extensive usage including gestational period. PAMAM dendrimers have great potential as carriers of anticancer drugs <sup>[8]</sup> and for gene delivery <sup>[9, 10]</sup>. In addition, dendrimer-based optical/paramagnetic Nano probes can cross the blood-brain barrier and be used for imaging of brain tumors <sup>[11]</sup>. Usage of PAMAM dendrimers during pregnancy may trigger transplacental transfer to fetus and infants were also exposed to PAMAM dendrimers from environment. In these cases, the assessment of the developmental neurotoxicity of PAMAM dendrimers is very important. Cytotoxicity studies *in vitro* have been performed using a human keratinocyte cell line <sup>[12]</sup> and human breast cancer cell lines <sup>[13]</sup>. The precise quantitative absorption and accumulation of nanoparticles was investigated after oral ingestion <sup>[14]</sup>. PAMAM dendrimers were capable of inducing cytokine production via the generation of reactive oxygen species, leading to a cytotoxic response in mouse macrophage cells <sup>[15]</sup>. However, the developmental neurotoxicity of PAMAM

exposure has not been adequately studied.

The effect of surface modifications to PAMAM dendrimers on their cytotoxicity has been studied previously <sup>[16, 17]</sup>, and amine-terminated (NH<sub>2</sub>) PAMAM dendrimers were associated with a higher cytotoxic response. The effect of PAMAM dendrimer generation on their cytotoxicity was also investigated using an *in vitro* experiment that examined high-generation (G4, G5, and G6) PAMAM dendrimers <sup>[12, 18, 19]</sup>. However, the wide range of PAMAM generations was not examined yet to elucidate the relationship between their generations and cytotoxicity. These studies were further conducted at equal molar concentrations, but did not consider increasing the total number of surface amines indicating the cytotoxicity with increasing generations.

### 1.3 Developmental neurotoxicity testing

Developmental neurotoxicity is any effect of a toxicant on the developing nervous system before or after birth that interferes with normal nervous system structure or function. The developing nervous system is especially susceptible to perturbations because development of the brain continues into the postnatal period and limited cell regeneration occurs following damage leading to persistent effects. Many chemicals in our environment have not been tested for toxicity to the developing brain and nervous system. Accumulating evidence indicates that many environmental toxicants are linked to neuronal disease, and some environmental toxicants are involved in developmental neurotoxicity (DNT) in humans and rodents

[20, 21]. It is well known that *in vivo* assays give more information about what is really happening inside organisms, while estimates based on two-dimensional *in vitro* observations might be very different from the actual *in vivo* situation. However, toxicity testing of chemicals in *in vivo* experimental studies has led to serious ethical concerns. Moreover, *in vivo* assays are too expensive to acquire batch dose data. Therefore, the development of alternative procedures and models is necessary. A three-dimensional (3-D) culture system has the advantages of being convenient, efficient and similar to the *in vivo* situation, with improved intercellular interactions, and the model is able to replicate basic processes of fetal brain development such as proliferation, differentiation and apoptosis [22, 23]. The use of human neurospheres, which are a kind of three-dimensional culture system likely to imitate the basic processes of brain development, has been a promising approach for DNT testing. The developing nervous system is highly vulnerable to the adverse effects of chemical agents. Therefore, a neurosphere culture system based on human neural progenitor cells (hNPCs) was developed and exposed the neurospheres to chemicals during neuronal development to detect DNT.

#### 1.4 Three-dimensional neurosphere

The neurosphere model 3-D neurosphere assays can simulate development of human nervous system and has the following advantages: convenient, efficient, similar to the *in vivo* situation, improves cell interactions, and reflects basic processes

of fetal brain development, including proliferation, differentiation, and apoptosis. *in vitro* assays (monolayer culture) are not sensitive and low precision. however, *In vivo* assay is too expensive to acquire batch dose data and has led to serious ethical concerns.

Previous studies have shown that the neurosphere model can be used to test developmental neurotoxicity. Differentiating Ntera2/clone D1 (NT2/D1) cell neurospheres were exposed to human teratogens such as acrylamide to test their developmental neurotoxicity [24]. The effect of valproic acid on neurodevelopment has also been studied by regulating gene expression and analyzing gene pathways [25]. In addition, the response of two anticonvulsant drugs on gene expression in human embryonic stem cells has been analyzed [26]. Neurosphere assays have been used to compare human and rat developmental neurotoxicity [27]. In this study, a 3-D neurosphere model based on human neural progenitor cells (hNPCs) was used to assess the developmental neurotoxicity of PAMAM dendrimers. PAMAM dendrimer have the potential to be used as drug carrier, the biodistribution and DNT are important. Therefore, the biodistribution of PAMAM dendrimers in the neurosphere and the effect of PAMAM dendrimer on neurosphere migration and differentiation was investigated. A fluorescence-labeled PAMAM dendrimers was used to investigate biodistribution in a 3-D cell culture model by exposing these dendrimers to 3-D neurospheres and found a time-dependent biodistribution of the dendrimers. To the best of my knowledge, this is the first study that evaluated the developmental

neurotoxicity of PAMAM dendrimer nanoparticles in a 3-D cell culture model.

## 1.5 Human neural progenitor cells

Human neural stem cells are self-renewing, multipotent cells that generate to neurons, astrocytes, and oligodendrocyte lineages through neural progenitor cells (NPCs) in vitro. During embryonic development, neural stem cells can generate the nervous system. Some neural stem cells in the adult brain can continue to produce neurons throughout life. Human NPCs (hNPCs) can differentiate into different types of neuronal cells in vitro (Fig 1-2). It has great potential for treating neurodegenerative diseases. Moreover, hNPCs are able to integrate into the host tissue and to differentiate into different neuronal subtypes [28, 29]. Therefore, hNPCs have been used as a new model system in screening assays for the effects of compounds on the development of the nervous system [30-32]. For biological markers of neurodevelopmental toxicities, it has been reported that receptor tyrosine kinase-like orphan receptor 1 (*ROR1*) modulates the growth of neurites and their branching pattern in hippocampal neurons [33]. The elevated levels of transforming growth factor, beta 1 (*TGFBI*) in ageing and neurodegenerative diseases have also been demonstrated [34]. The basic functions of the pro-neural gene, neurogenin 1 (*NEUROG1*), have been elucidated; it plays an important role in regulating the development of the olfactory system [35], and in neocortical development [36]. In this

thesis, hNPCs was differentiate to neurons to culture a neurosphere, chemicals were exposure during hNPCs differentiation to simulate chemicals exposure on developing human nerve system.

## 1.6 Innovative point and structure in this thesis

Innovation points in this thesis are two things that a novel 3-D culture system using hNPCs for DNT assessment was developed and DNT of PAMAM dendrimer nano-particles were tested using this system. The structure of this thesis shows bellow.

### Chapter 1 Introduction

In this chapter, the background of this research was introduced, including Human neural progenitor cells, Three-dimensional neurosphere, developmental neurotoxicity, and Polyamidoamine (PAMAM) dendrimers. Motivation and the structure of this study were also addressed.

### Chapter 2 Optimization of neurosphere assays

In this chapter, neurospheres system formed from human neuronal progenitor cells (hNPCs) was established for risk evaluation of chemical exposure.

### Chapter 3 Developmental neurotoxicity testing of nano-particle.

In this chapter, neurotoxicity of PAMAM dendrimer nano-particle was tested using neurospheres system

### Chapter 4 Conclusions and future researches

In this chapter, the main results are summarized. In particular, the future research

points was also directed.

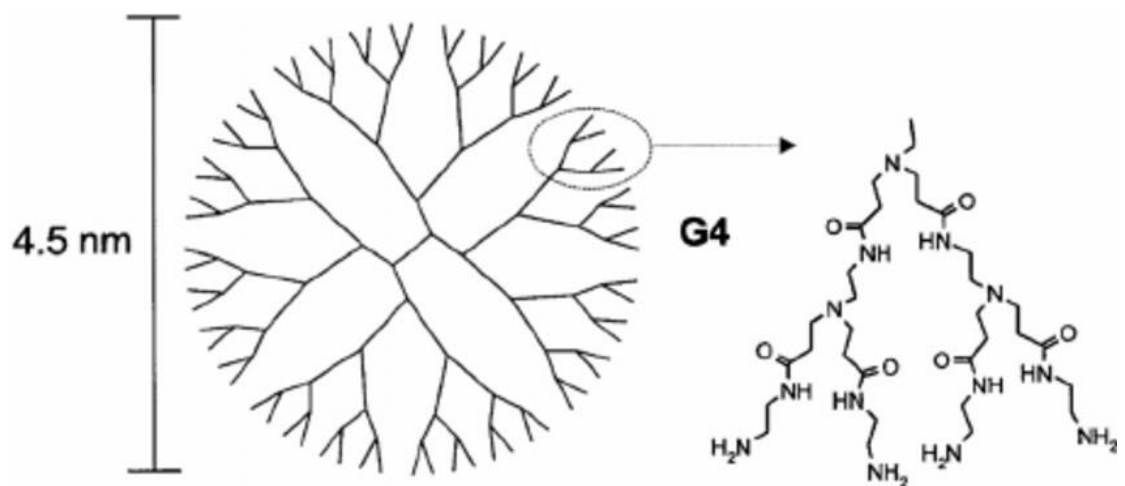
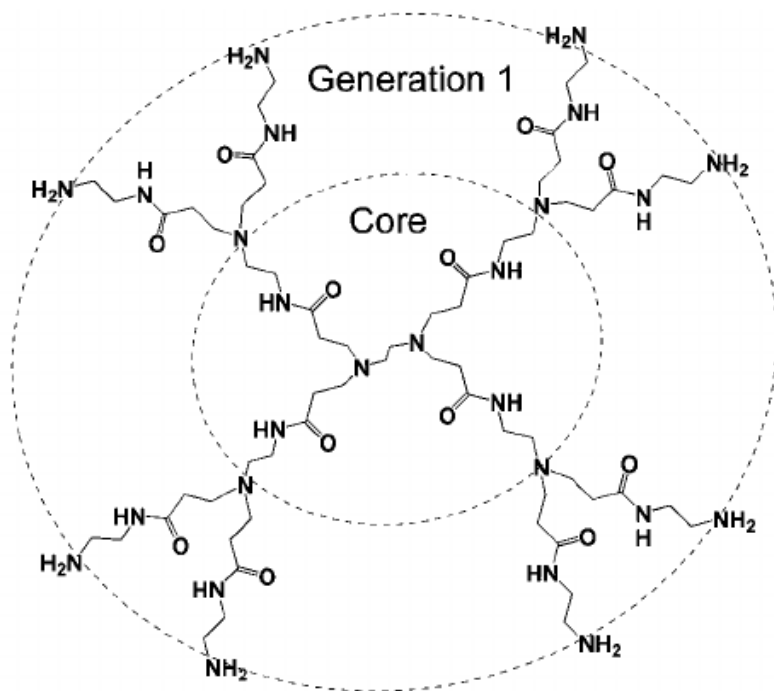


**Fig. 1-1** Structure of PAMAM dendrimer generation 1 and generation 4.

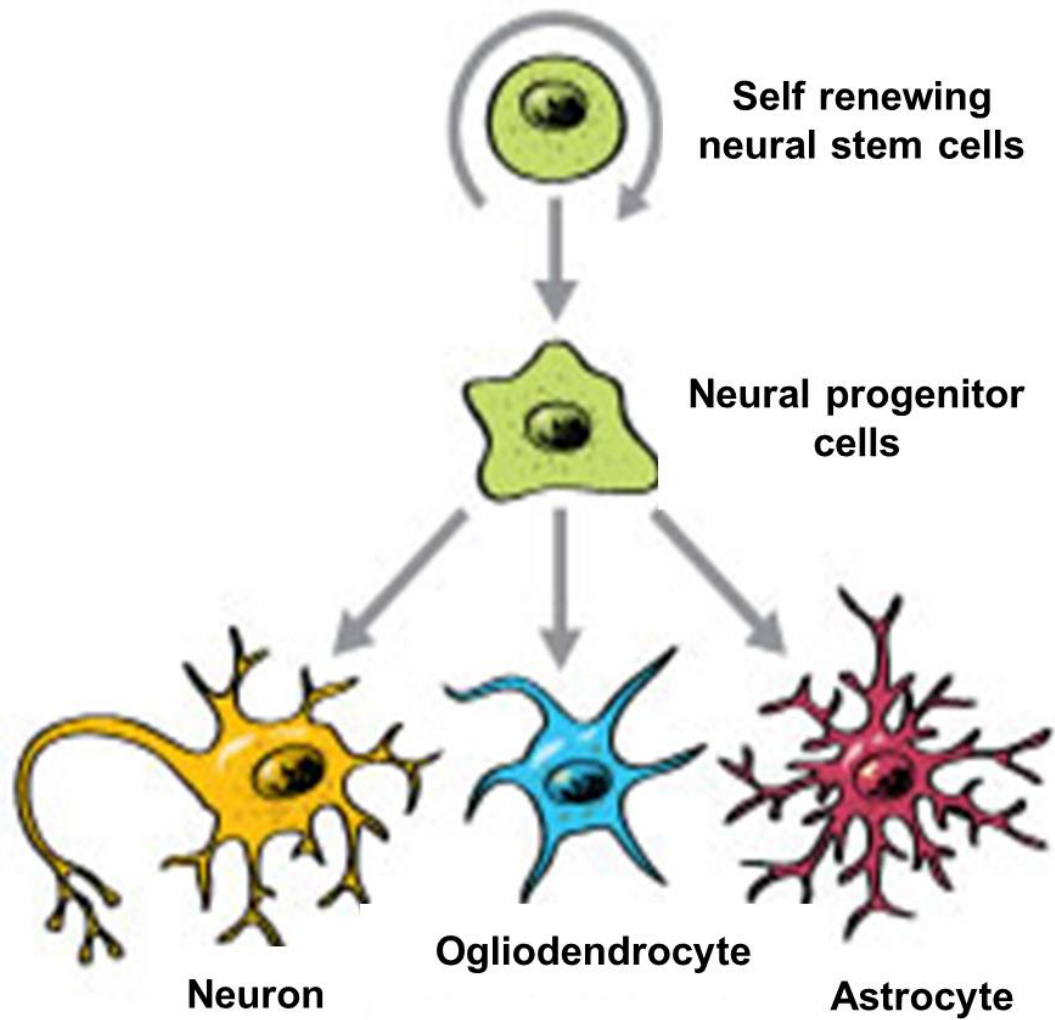


**Fig. 1-2** Human neural progenitor cells (hNPCs) can differentiate into different types of neuronal cells.

## Chapter 2 Optimization of neurosphere assays for developmental neurotoxicity testing

### 2.1 Introduction

Accumulating evidence indicates that many environmental toxicants are linked to neuronal disease, and some environmental toxicants are involved in developmental neurotoxicity (DNT) in humans and rodents [20, 21]. It is well known that *in vivo* assays give more information about what is really happening inside organisms, while estimates based on two-dimensional *in vitro* observations might be very different from the actual *in vivo* situation. However, toxicity testing of chemicals in *in vivo* experimental studies has led to serious ethical concerns. Moreover, *in vivo* assays are too expensive to acquire batch dose data. Therefore, the development of alternative procedures and models is necessary. A three-dimensional culture system has the advantages of being convenient, efficient and similar to the *in vivo* situation, with improved intercellular interactions, and the model is able to replicate basic processes of fetal brain development such as proliferation, differentiation and apoptosis [22, 23]. The use of human neurospheres, which are a kind of three-dimensional culture system likely to imitate the basic processes of brain development, has been a promising approach for DNT testing [37, 38]. The developing nervous system is highly vulnerable to the adverse effects of chemical agents. Therefore, a hNPCs-based neurosphere culture system was developed and chemicals were exposed to the neurospheres during the neuronal development to verify whether this system can be used to detect DNT.

The basement membrane (BM) is a key component of a neurosphere testing model. The three-dimensional system basement membrane provides a scaffold for neuronal cell differentiation and is known to regulate adhesion, migration, proliferation and differentiation [39]. Poly-L-Ornithine (PLO), a highly positively charged amino acid chain, is generally used as a coating reagent to promote cell adhesion in culture. PLO alone or in combination with Fibronectin or Laminin-I is frequently used to enhance attachment and differentiation of various types of neurons and neural stem cells [40, 41]. Laminins synthesized membrane surfaces has a highly integrated structure composed of extracellular matrix (ECM) molecules, develop niche microenvironment inducing an activation of transcellular membrane signals transmission in neuronal cells differentiation. Laminins are the major cell-adhesive proteins in the basement membrane, consisting of three subunits termed alpha, beta and gamma [42]. In this study, it was attempted to acquire the efficient progenitor cells derived neurite outgrow on a substrate that integrates several laminin subunits including Laminin 511 (LM511) and Laminin 111 (LM111). LM511 is the most widely expressed laminin in the body [43]. The human ES cell membrane has high affinity for intact LM511, which is effective for maintaining pluripotency, supporting efficient adhesion and expansion of dissociated human pluripotent stem cells [44]. LM111 is present in the early embryo and later in certain epithelial cells, but it is a rare isoform in vivo [45, 46]. Neurite differentiation protocols enable the creation of different subtypes of neurons to study fate decision pathways [47], and have further

utility as assay systems to detect adverse effects of toxicity in neuronal development.

Two chemicals were exposed in the novel culture system to find out whether it can be used to evaluate developmental neurotoxicity. Benzo[a]pyrene (BaP), a well known carcinogen, is widespread in the environment. Although the neurotoxic effect of BaP has not drawn much attention, adverse effects of BaP on learning and memory have been reported <sup>[48]</sup>. Neuronal apoptosis plays a major role in BaP-induced neurotoxicity <sup>[49]</sup>. 5-Azacytidine (5AZ) is a potent inhibitor of DNA methylation <sup>[50]</sup>. It has been reported that 5AZ induces toxicity in PC12 cells and in rat brain, however, no neurotoxicity has been found <sup>[51, 52]</sup>.

## 2.2 Materials and methods

### 2.2.1 Chemicals

L-glutamine, Poly-L-ornithine and laminin from engelbreth-holm-swarm (LM111) were provided by Sigma-Aldrich (Tokyo, Japan). Human recombinant laminin (LM511) was obtained from BioLamina AB (Stockholm, Sweden). Benzo(a)pyrene and 5-Azacytidine was bought from Schell Chemical (Co, New York, N. Y).

### 2.2.2 hNPC sphere formation and neural cell differentiation on the extracellular matrix

The human neuronal progenitor cells (hNPCs), derived from H9 human embryonic stem cells, were obtained from Chemicon-Millipore (ENStem Human

Neural Progenitor Expansion Kit; Norcross, GA). For hNPC proliferation prior to the neural progenitor sphere (NPS) formation, preparations were incubated in poly-L-ornithine/LM111-coated 60-mm Petri dishes with NEM medium (ENStem-A Neural Expansion Medium(EMD Millipore, Japan) with Glutamine and FGF-2 supplement solution) and then hNPCs were seeded at a density of  $2 \times 10^6$  cells/dish and incubated for 4 days. Preparations were then dissociated with accutase dissociation solution (ICT, FUAT104). Procedures of neurosphere culturing was show in Fig 2-1, sphere were formed from day0 to day 5, NPS formation was conducted in Nunc low cell binding 96-well plates (Thermo Fisher Scientific Inc., Waltham, MA) with a density of  $6 \times 10^3$  cells/well in NEM medium. In the final step, NPS were transferred and seeded to 48-well plates in which the wells were coated with LM511 (BioLamina AB), a mixture of LM511 and LM111 (LM511+LM111), or mixture of poly-L-ornithine, LM111 and LM511 (PLO/LM511+LM111), or a combination of poly-L-ornithine and LM111 (PLO/LM111), separately. The wells contained Neurobasal (Gibco,Japan) medium containing 5 units/ml penicillin with 5  $\mu$ g/ml streptomycin and Gibco supplement B27 (1/50), Glutamax-1(1/100, Gibco), N2 (1/100, WAKO,Japan) and BDNF (1/1000, Gibco). The spheres were continuously cultured for at least 5 days to induce mature neural cells.

### 2.2.3 Immunohistochemistry staining

Neurospheres were fixed with 4% paraformaldehyde for 15 min at RT, and permeabilized by incubation for 30 min in 0.1% Triton X-100 (SigmaAldrich,

Japan)PBS. After blocking non-specific binding with 0.1% bovine serum albumin (BSA) in PBS, the fixed neurospheres were incubated with primary antibodies (MAP2 monoclonal, SigmaAldrich, Japan) overnight at 4°C, and then for 1 h at 37 °C with goat anti-mouse IgG antibodies conjugated to Alexa Fluor 568 (orange fluorescent dye, Invitrogen, Life Technologies, USA) or Alexa Fluor 488 (green fluorescent dye, Invitrogen, Life Technologies). The neurospheres were then incubated with Hoechst 33342 work solution (Molecular Probes, Life Technologies) for 15 min at RT. The staining was visualized with a fluorescent microscope (Olympus IX70, Olympus Corporation, Tokyo, Japan).

#### 2.2.4 Image analysis for neurite outgrowth

Sphere area and neurite migration were investigated. Images for each neurosphere were acquired with a 10 x lens, and radii of the core (R1) and sphere (R2) were measured using Image J. Corona areas were calculated (area of R2 minus area of R1). For determination of neurite length/cell, the IN Cell Analyzer 1000 (GE Healthcare, Japan) was used to automatically acquire fluorescent images. 20 images obtained with a 10 x lens were used to analyze neurite length. Cell images were analyzed using IN Cell Developer box (GE Healthcare). Cellular nuclei were first segmented and counted using the Hoechst channel. The neuron cell bodies were then segmented and their associated neurites were identified using the MAP2 channel. Neurite length was identified for each cell body and neurite length/cell was calculated.

## 2.3 Results

### 2.3.1 Neurosphere formation and differentiation

To develop a neurosphere differentiation culture system, it was utilized a three-dimensional embryoid aggregate protocol to examine neurosphere formation and differentiation using various types of coating matrices. Fig. 2-2 A is the timeline schematic for this protocol, in which neuronal progenitor sphere(NPS) were formed by Day 5 and neural maturity was induced by Day 10. Neurospheres and expanding single layer hNPC coronas were formed on all types of membrane-coated surfaces by Day 8. The expanded corona area of neurosphere was observed in PLO/LM111 coated surfaces, but the neurosphere central area was weak and not well attached on coating surfaces at Day 10 (Fig. 2-2B). Comparing the three other types of coating membranes at Day 10, significant neurosphere expanding corona areas were observed in the PLO/LM511+111 coated surface (Fig. 2-2B). The neurosphere expanding corona areas were significantly increased in PLO/LM511+111 surface on Day 10 compared with other coating systems (Fig. 2-3). However, the corona areas were too expanded and not stable, suggesting that the PLO/LM511+111 surface is not suitable for neurotoxicity testing. For further investigation of the expanding corona region, the neurite length/cell were analyzed, however, no significant differences were found for neurite length/cell (Fig. 2-5).

### 2.3.2 Benzo[a]pyrene and 5-Azacytidine exposure

To investigate whether the LM511 coating is appropriate for assessment of neurotoxicity of chemicals, neurospheres on LM511-coated surface were exposed to benzo[a]pyrene (BaP) and 5-Azacytidine (5AZ) from Day 2 to Day 5 (Fig. 2-6A). BaP at a concentration of 10  $\mu\text{g/ml}$  significantly inhibited expanding corona areas (Fig. 2-7A). However, BaP did not affect neurite length/cell at any test concentrations (Fig. 2-7 B). 5AZ at a concentration of 0.3  $\mu\text{g/ml}$  significantly inhibited expanding corona areas, while no significant differences from controls were found for lower concentrations (Fig. 2-9A). However, no significant changes were found for neurite length/cell at test concentrations (Fig. 2-9B).

## 2.4 Discussion and summary

The aim of this section was to determine an optimal basement membrane culture system and establish a neurosphere model to detect developmental neurotoxicity. A novel, efficient three-dimensional culture system for neurosphere formation and neuronal differentiation was developed with a combination of neurosphere formation on U-bottom plates and differentiation on the extracellular matrix.

Several kinds of coating system were tested. The neurosphere expanding corona areas were significantly increased on PLO/LM511+111 surface on Day 10. The extended neuron was too much compare with other coating system. Moreover, the standard deviation value was high, suggesting that the PLO/LM511+111 surface is

not as stable as the LM511 and is not suitable for neurotoxicity testing. The results suggest that neurospheres can be maintained and appropriately differentiated when cultured using a LM511 or LM511+LM111 coating system. The LM511-coated surface system is more efficient and easier to operate than LM511+LM111 coating system, therefore it is suggested that LM511 is the best coating system. Culture systems using LM511 have been reported previously <sup>[53]</sup>. hES/iPSCs 2-D culture system were well established under LM511 coating surface. Basement membrane components play an important role in supporting the regional-specific differentiation of embryonic stem cells into hepatic endoderm. Using an HEK293 cell line (rLM10-293 cells) stably expressing LM511, embryonic stem cells could be induced to differentiate into definitive endoderm and subsequently into pancreatic lineages <sup>[54]</sup>. Instead of using cell-generated LM511, a commercially produced LM511 was used to establish a culture system. An efficient three-dimensional culture system for NS formation and neuron differentiation was developed. This novel NS culture system was used to assess neurotoxicity in previous study <sup>[55]</sup>.

It has been shown recently that Benzo[a]pyrene may induce neurotoxicity <sup>[56, 57]</sup>. However, 5AZ can only induce acute toxicity in the nervous system via apoptosis <sup>[50, 58, 59]</sup>. Therefore, two chemicals were used to evaluate the novel model to determine whether it can assess neurotoxicity. It was found that both chemicals inhibit corona areas of neurospheres, suggesting that both chemicals may influence cell migration. BaP induced decreases of neurite length/cell at concentrations of 1 µg/ml and 10

$\mu\text{g/ml}$  However, 5AZ induced significant increases in neurite length/cell at a concentration of 0.3  $\mu\text{g/ml}$ . It is suggested that BaP but not 5AZ induces neurotoxicity by inhibiting neurite differentiation. The increased neurite length/cell may be because of the decreased cell number.

The results revealed that a LM111 coating system cannot support the neurospheres for long enough. A PLO/LM511+LM111 coating system showed the best attachment, however, the neurospheres that formed were too extended to make a stable system. The LM511 and LM511+LM111 coating systems showed similar performance, but LM511 strongly supported neurosphere culture for long periods. hNPCs showed the ability to differentiate to neuronal cells and neurites were well developed on a LM511-coated surface.. Therefore, it is suggested that LM511 single coating is best for establishing a stable and efficient culture system. Both BaP and 5AZ inhibited cell migration. BaP, but not 5AZ, inhibited neuronal differentiation. It is suggested that this neurosphere model can be used to evaluate developmental neurotoxicity. Neuron migration can be analyzed by measurement of expanding corona areas. Neurite differentiation can be quantified by measuring neurite length/cell.

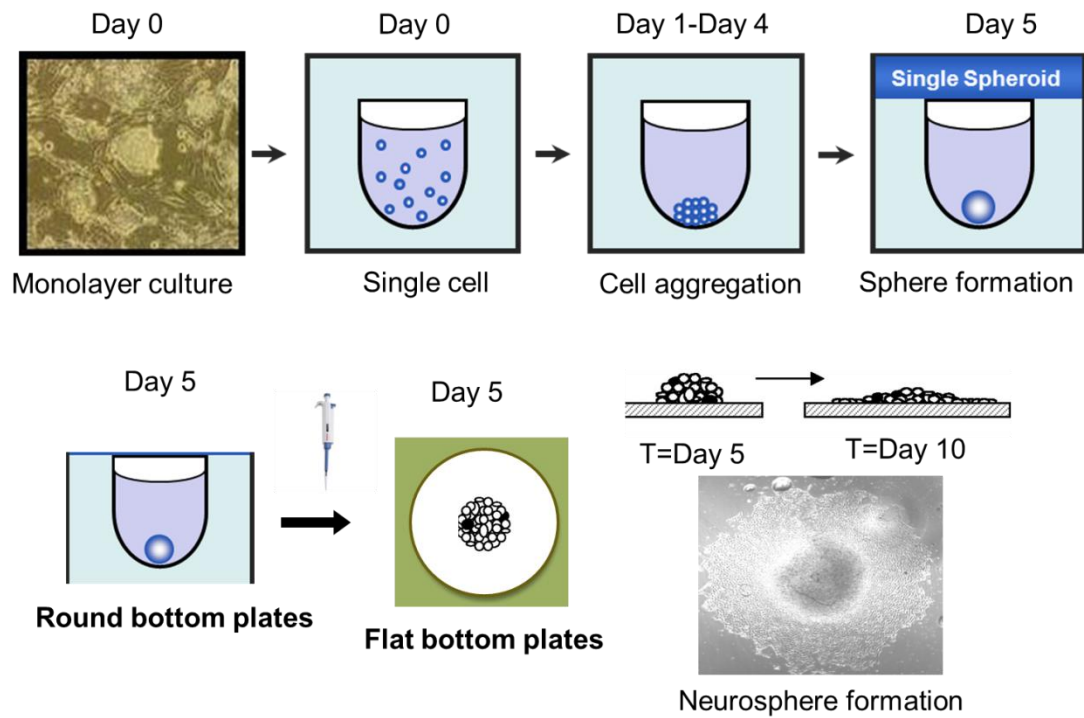


**Fig. 2-1** Procedures of neurosphere culturing. Spheres were formed from day 0 to day 5 in 96-well plates with round bottoms, and then transferred and seeded to 48-well plates in which the wells were coated with BM, separately. Further, spheres were continuously cultured for another 5 days at least to induce mature neural cells.

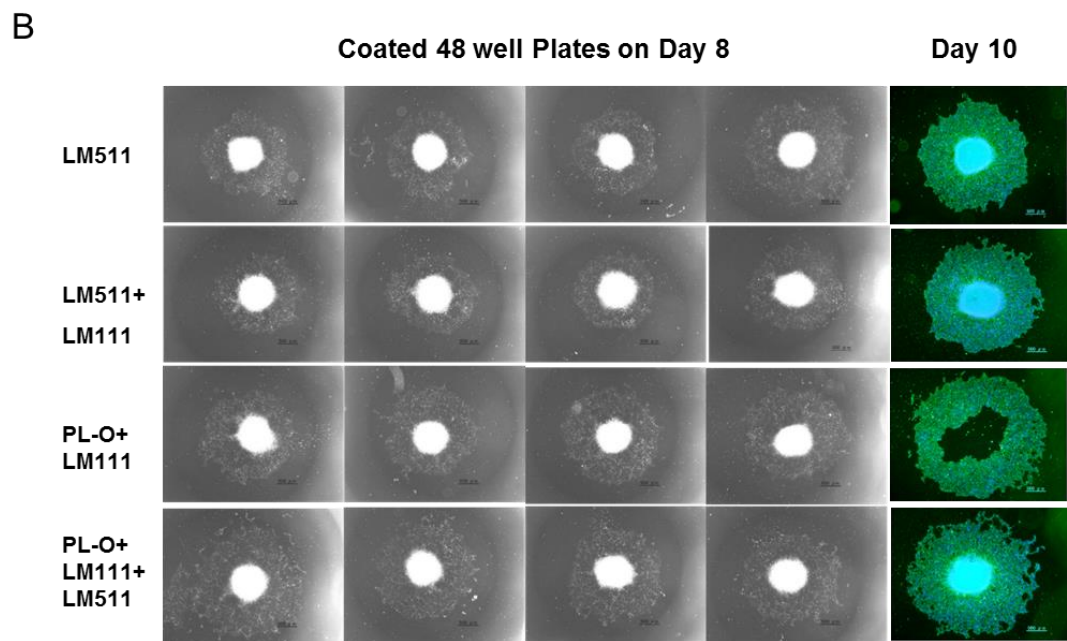
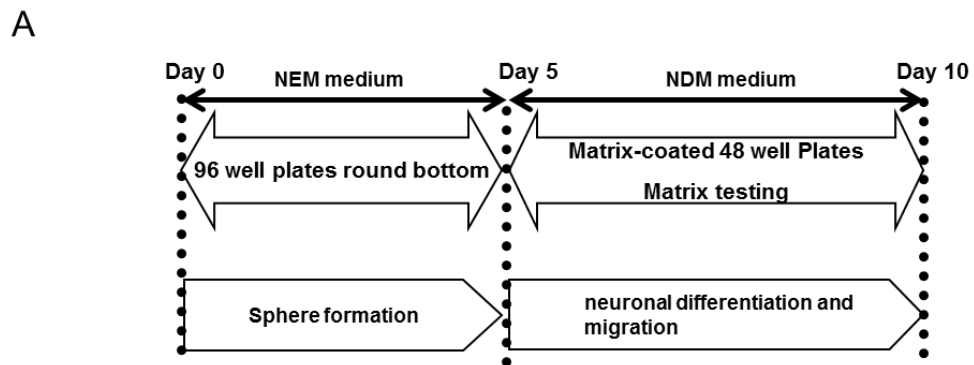


**Fig. 2-2** Culture schedules (A) and photographs (B) of sphere formation, differentiation and migration. Sphere formation was conducted as described as Fig. 2-1. Images of neurospheres shows Spheres, which were cultured with different matrices on Day 8 and Day 10.

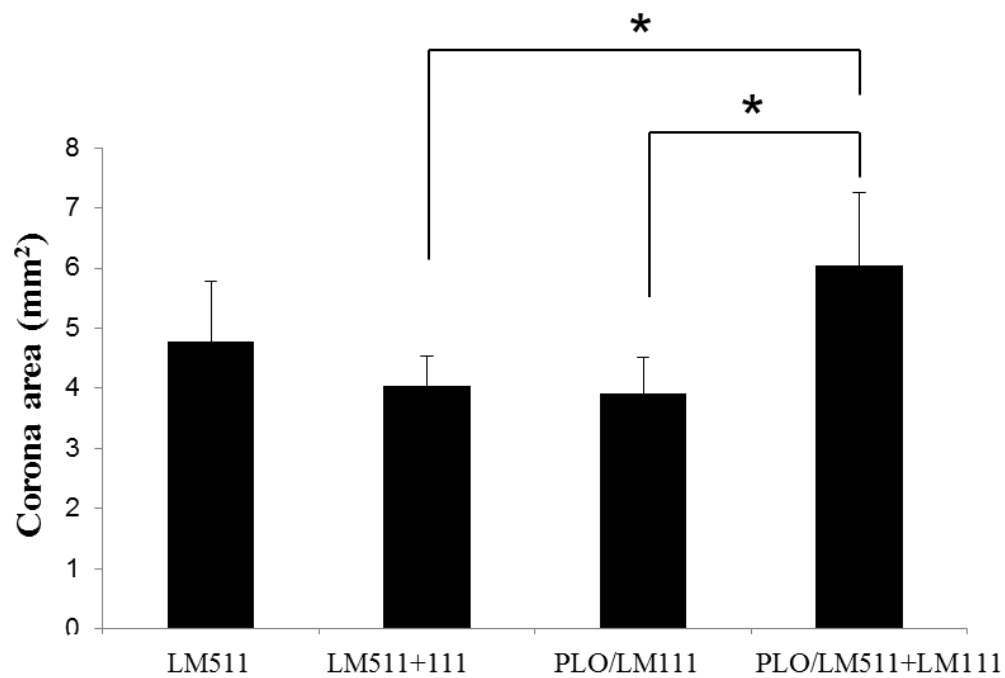


**Fig. 2-3** Quantitative analysis of expanding corona area neurospheres (R2-R1), examined by fluorescence microscopy. Data are expressed as mean  $\pm$  SD for three independent experiments.  $*P < 0.05$  was considered to be statistically significant differences between groups using ANOVA followed by tukey.

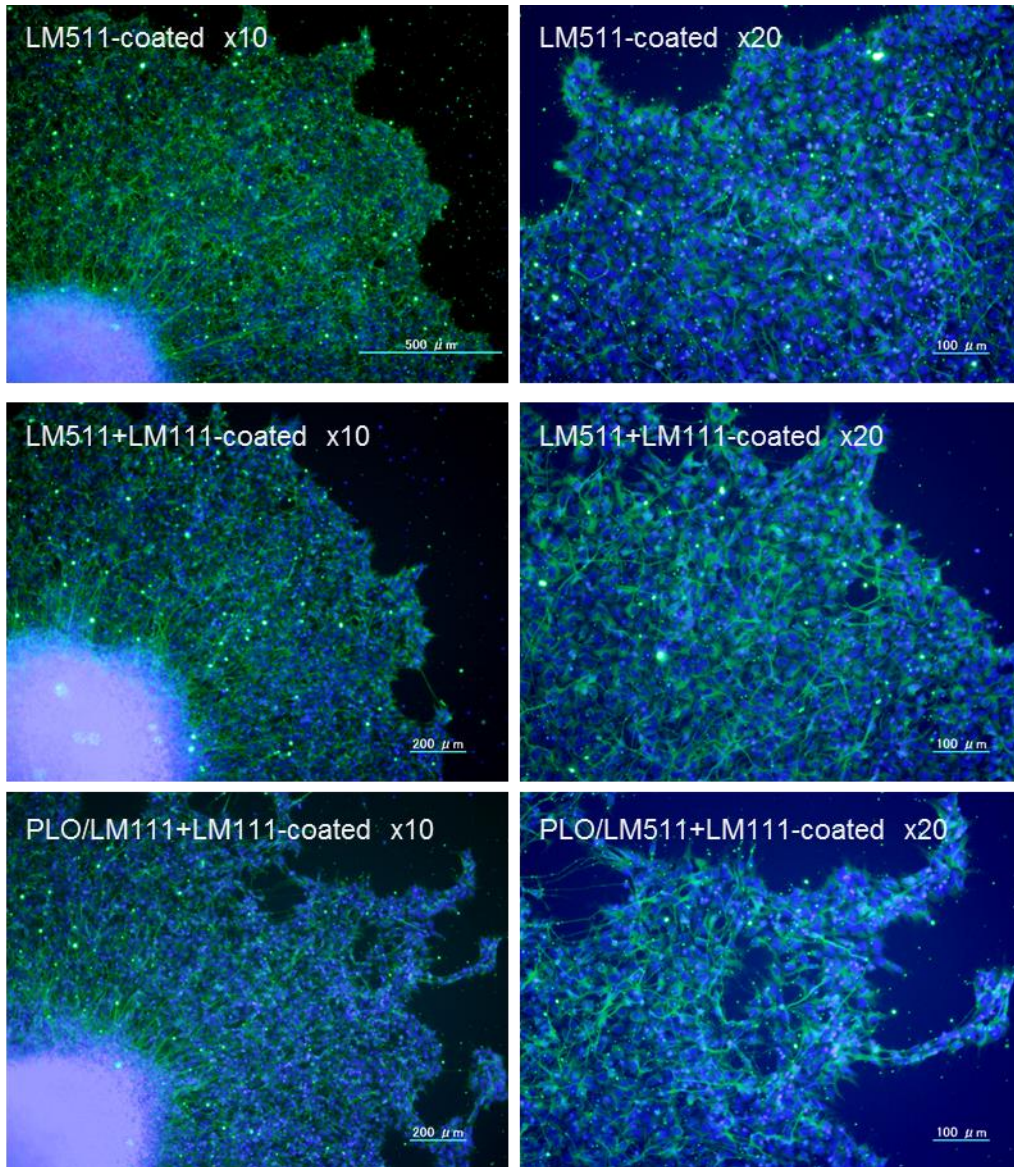


**Fig. 2-4** Immunofluorescence of MAP2-positive hNPCs at expanding corona on LM511-coated plates, LM511+LM111-coated plates and PLO/LM511+LM111-coated plates. Cells were stained with hoechst33342 (blue) and Alexa 488-conjugated anti-MAP2 (green).

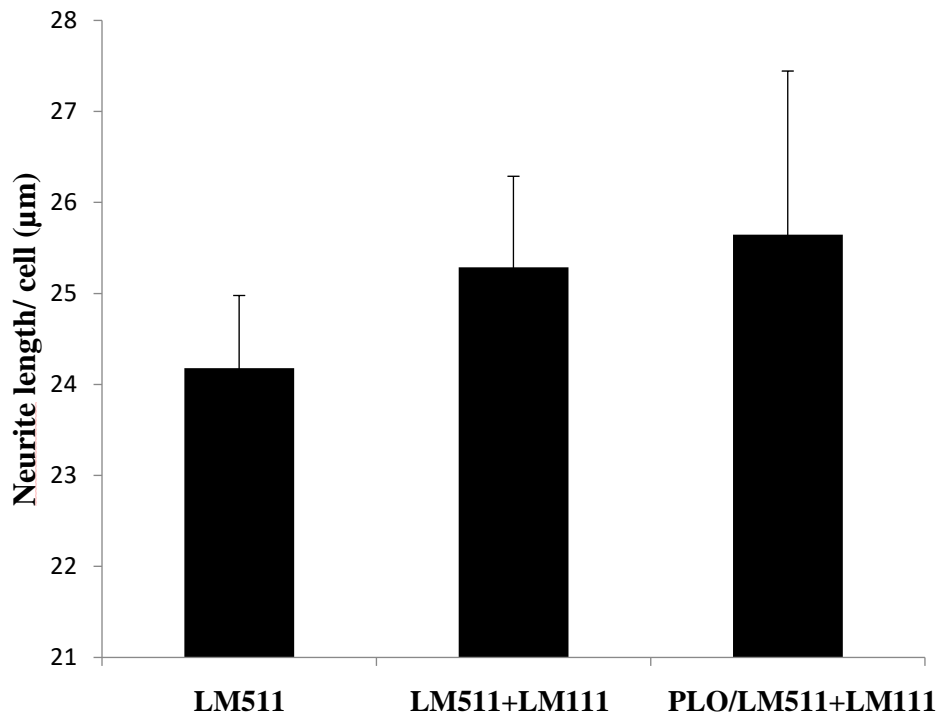


**Fig. 2-5** Typical outgrowth of neurosphere. Quantitative analysis of neurite length / MAP2-positive cell and nuclei member counting. Data are expressed as mean  $\pm$  SD for three independent experiments. Significant differences between groups using ANOVA followed by tukey.

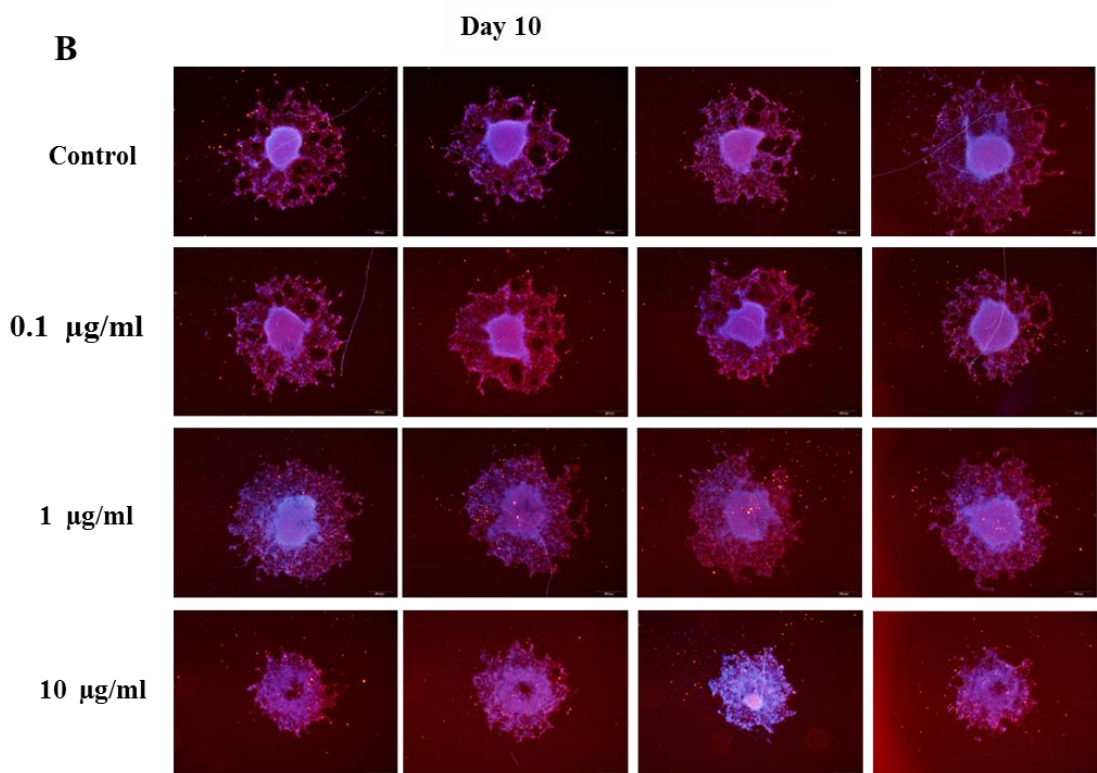
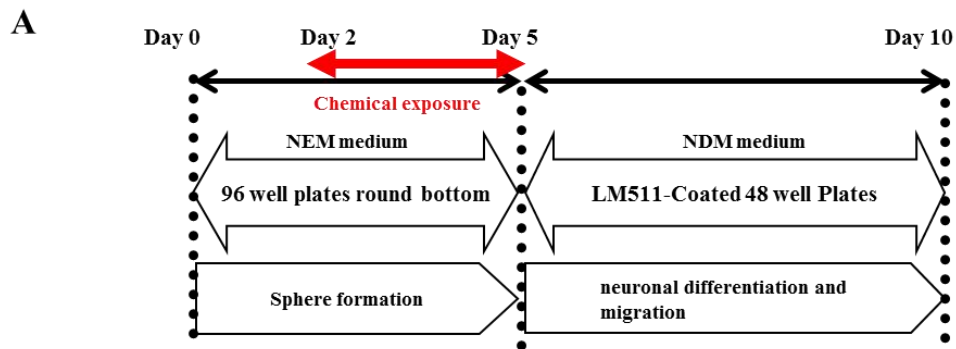


**Fig. 2-6** Schematic of chemical exposure of neurospheres (A). hNPC were incubated with chemicals from Day 2 to Day 5 in 96-well plates with round bottoms. To compare four different coating membrane in day 10, cells were stained with hoechst33342 (blue) and MAP2 (Alexa 568, red). Typical outgrowth of neurosphere exposed to BaP, four parallel spheres were tested for each concentration (B).

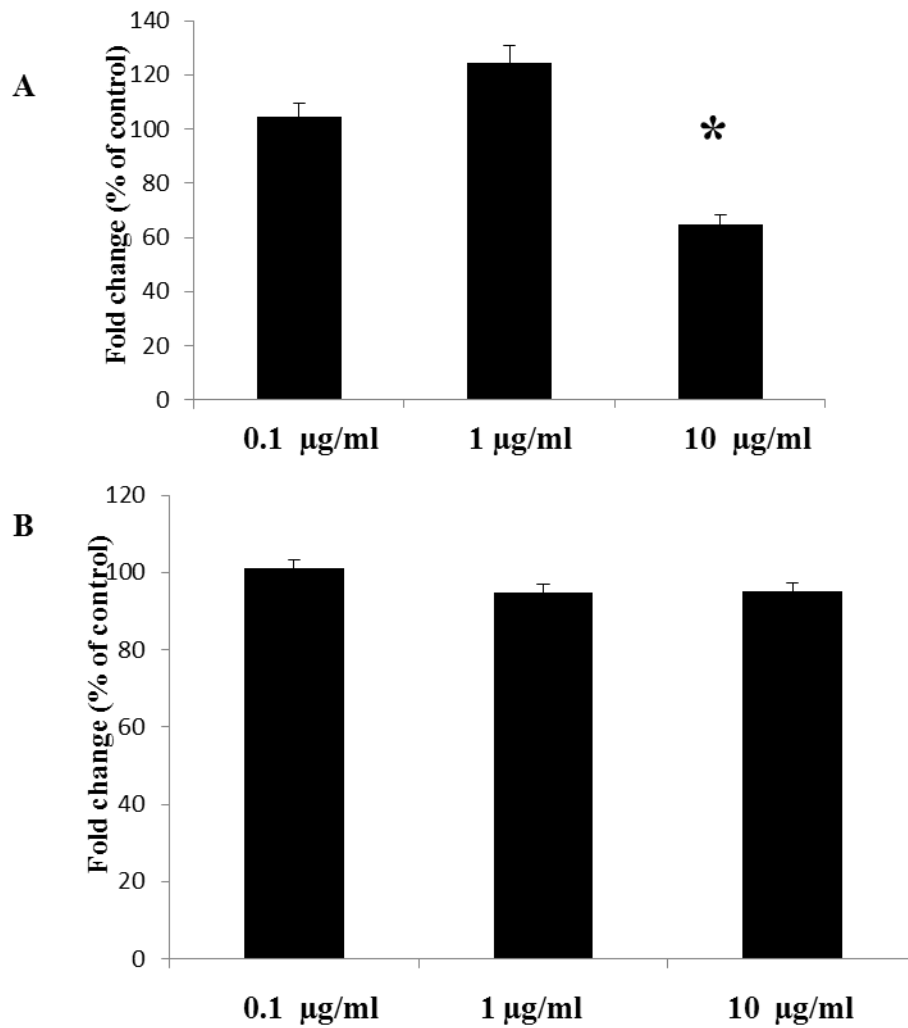


**Fig. 2-7** Quantitative analysis of exposed to BaP at concentrations of 0.1- 10 µg/ml for corona area (A). Quantitative analysis for neurite length / MAP2-positive cell and nuclei member counting (B). Data are expressed as the percentage of the control  $\pm$  SD for three independent experiments.  $*P < 0.05$  was considered to be statistically significant differences between the treatment group and the vehicle control using ANOVA followed by dunnett's post hoc test.

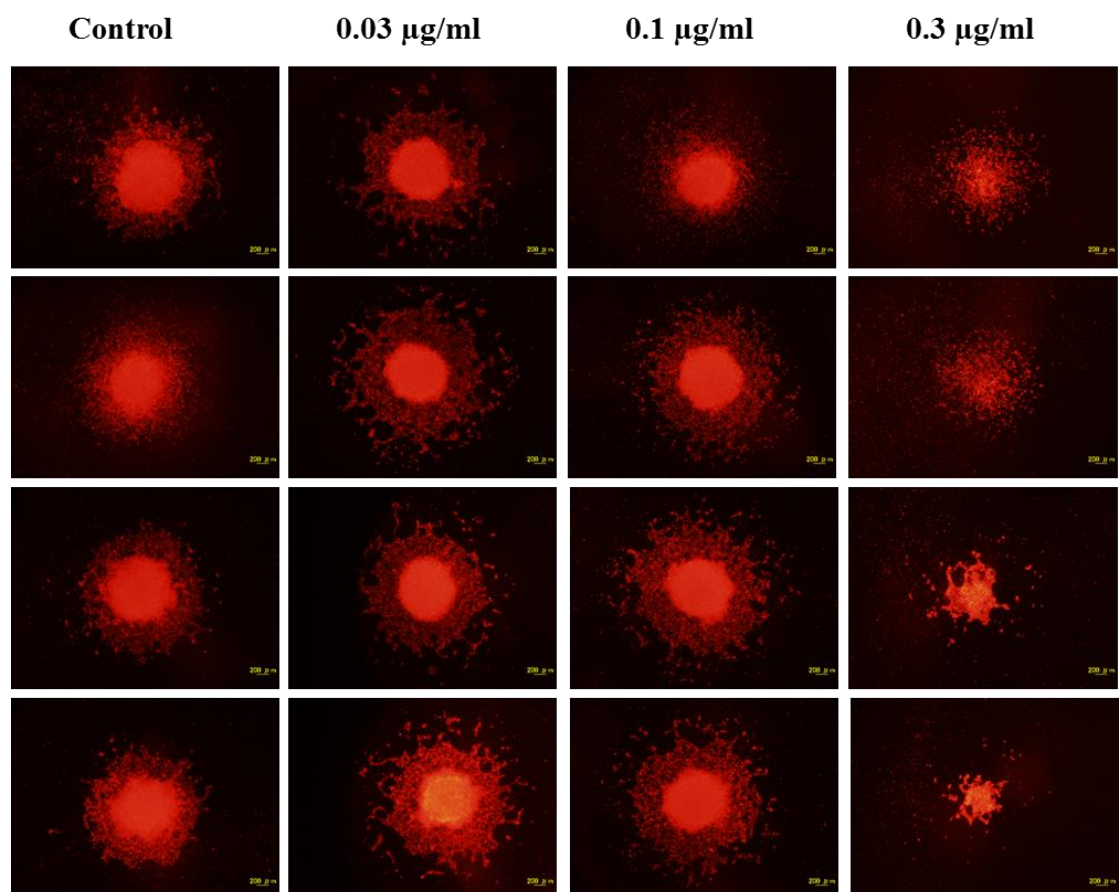


**Fig. 2-8** Typical outgrowth of neurosphere exposed to 5AZ. Cells were stained with MAP2 (Alexa 568, red). Four parallel spheres were tested for each concentration.

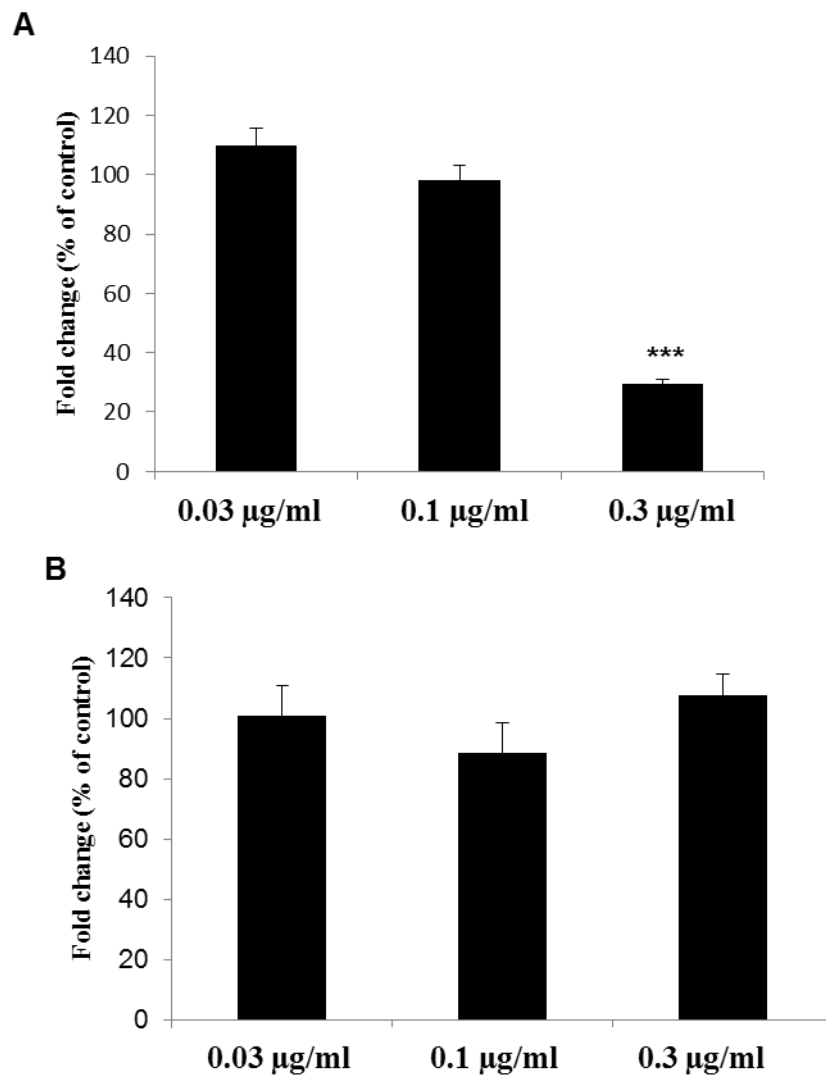


**Fig. 2-9** Quantitative analysis of exposed to 5AZ at concentrations of 0.03-0.3 µg/ml for corona area. (A) Quantitative analysis for neurite length / MAP2-positive cell and nuclei member counting. (B) Data are expressed as the percentage of the control  $\pm$  SD for three independent experiments. \*\*\*P < 0.001 were considered to be statistically significant differences between the treatment group and the vehicle control using ANOVA followed by dunnett's post hoc test.

# **Chapter 3 Effects of PAMAM dendrimers nanoparticles on neurosphere**

## **3.1 Introduction**

Polyamidoamine (PAMAM) dendrimers nanoparticles are a common type of dendrimers that have a radial structure consisting of a 2-carbon ethylenediamine core and functional groups on their surfaces. These functionalized surface groups can be easily changed, enhancing their wide use for biological applications such as drug <sup>[8]</sup> or gene delivery <sup>[9, 10]</sup>. PAMAM dendrimer can be synthesized from generation 0 (G0) to generation 10 (G10). The size of PAMAM dendrimers were increased with increasing generation. The probability of human exposure to PAMAM dendrimers during infancy may increase because of their potential usage, and developing nervous system is highly vulnerable to the adverse effects of chemical agents. Moreover, in order to use PAMAM dendrimers as drug carrier to treat brain disease, PAMAM need to reach parenchyma of brain. In these cases, the assessment of the developmental neurotoxicity of PAMAM dendrimers is very important. In this section, DNT of two kinds of generation 4 PAMAM dendrimers were assessed: positive charged PAMAM-NH<sub>2</sub> and natural charged PAMAM-SC (sodium carboxylate).

To assess PAMAM dendrimer toxicity on human brain after intracerebroventricular injection, firstly, in vitro study is needed to study neurotoxicity of PAMAM dendrimers on neuron cells. Previous studies have shown that the embryonic stem cells model can be used to test developmental neurotoxicity. The effect of valproic

acid on neurodevelopment has also been studied by regulating gene expression and analyzing gene pathways. However, most of agents cannot be identified with certainty. This is because 2-D models do not reflect basic processes of fetal brain development. Therefore, 3-D neurosphere model should be used. The neurosphere model has the following advantages: convenient, efficient, similar to the *in vivo* situation, improves cell interactions, and reflects basic processes of fetal brain development, including proliferation, differentiation, and apoptosis. Differentiating Ntera2/clone D1 (NT2/D1) cell neurospheres were exposed to human teratogens such as acrylamide to test their developmental neurotoxicity [24]. The effect of valproic acid on neurodevelopment has also been studied by regulating gene expression and analyzing gene pathways [25]. In addition, the response of two anticonvulsant drugs on gene expression in human embryonic stem cells has been analyzed [26]. Neurosphere assays have been used to compare human and rat developmental neurotoxicity [27]. In this section, the neurosphere model was used to assess the neurotoxicity of PAMAM dendrimers. The migrated cell from neurosphere core was investigated, It was also investigated the biodistribution of PAMAM dendrimers in the neurosphere and the effect of PAMAM dendrimer on neurosphere. A fluorescence-labeled PAMAM dendrimers was used to investigate biodistribution in a 3-D cell culture model by exposing these dendrimers to 3-D neurospheres and found a time-dependent biodistribution of the dendrimers. To the best of my knowledge, this is the first study that evaluated the developmental neurotoxicity of PAMAM dendrimer nanoparticles in a 3-D cell culture model.

## 3.2 Materials and methods

### 3.2.1 Dendrimers and test chemicals

PAMAM (ethylenediamine core, generation 4.0; Cat. No. 664049-1KT) 10 wt.% methanol solution and PAMAM G4-SC which was modified with sodium carboxylate surface groups (10 wt. % in methanol, 412430-2.5G) were purchased from Sigma-Aldrich (St. Louis, MO, USA). PAMAM was conjugated with an Alexa546 fluorophore to prepare infrared-labeled PAMAM dendrimers. Conjugation has been synthesized via an amide bond between the primary amine of the dendrimer and the N-hydroxysuccinimide-activated carboxyl of the fluorophore. 20 mg of PAMAM G4 stock solution was combined with 0.1 M Alexa Fluor 488 or Alexa Fluor 546 carboxylic acid, succinimidyl ester (Invitrogen., Eugene, Oregon, USA) at pH 8.3. The reaction was allowed to proceed under stirring for 3 hours in RT. The product was purified using a Slide-A-Lyzer Dialysis Cassette (Thermo Scientific., USA) with 3500 Dalton cut off to remove free fluorophore.

### 3.2.2 Reagents for cell-based assays

Neural expansion media (NEM) were obtained from ENStem-A. Neurobasal medium and Glutamax were purchased from Life Technologies (Gibco; USA). hNPCs derived from H9 human embryonic stem cells were obtained from Chemicon-Millipore (ENStem Human Neural Progenitor Expansion Kit; Norcross, GA, USA).

### 3.2.3 Neurosphere formation and Incorporation of Alexa-labeled PAMAM

hNPCs were cultured in NEM supplemented with 0.05% b-FGF and 1% L-glutamine on poly-ornithine-coated and LM111-coated dishes. On day 0 (d0), the cells were transferred to 96-well round bottom plates (Nunc, Falcon) at a density of 6,000 cells per well to allow neurosphere formation, this 3-D culture system has been established in previous study (Zeng et al., 2015).

Alexa546-labeled PAMAM dendrimers at a concentration of 10  $\mu\text{g/ml}$  were incubated with neurospheres in 96-well round bottom plates at day 2. The spheres were transferred to a LM511-coated glass bottom dish for observation at day 3, day 4, and day 5. Microphotographs showing the incorporation of Alexa546-labeled PAMAM dendrimers were obtained using an Olympus LV1200 High-Performance Laser Scanning Microscope (Olympus Optical, Japan). Images for illustration were obtained using 10 $\times$  and 20 $\times$  objectives. The 3-D images were created by FV10-ASW software (Olympus Optical, Japan) using 7 images per stack. The thickness for each stack was 3 $\mu\text{m}$ .

### 3.2.4 Immunofluorescence and morphological analysis

To investigate neurosphere proliferation, migration and differentiation, on day 2 (d2), 3 doses of PAMAM dendrimers (1  $\mu\text{g/ml}$ , 3 $\mu\text{g/ml}$  and 10  $\mu\text{g/ml}$ ) were exposed for 72 h in NEM and NDM, respectively.

On day 5 (d5), neurospheres were transferred in NEM (ENStem-A) supplemented with 0.05% b-FGF and 1% L-glutamine (Sigma-Aldrich, St. Louis, MO,

US) on poly-ornithine-coated (Sigma-Aldrich, St. Louis, MO, US) and LM111-coated (Sigma-Aldrich, St. Louis, MO, US) 48-well plates. At day 7, Plus EdU Alexa Fluor imaging kits (Thermo fisher scientific, Tokyo, Japan) was used to label newly synthesized DNA in hNPCs for 24 h. At day 8, cells were then treated with 2 g/ml of Hoechst 33342 solution for 15 min at room temperature to label all cell nuclei. Immunofluorescence images were acquired using FV1200 (Olympus, Tokyo, Japan). Sphere area was investigated using Image J. Sphere was identified manually and area was calculated by software.

To investigate neurosphere differentiation, the neurospheres were gently transferred to a 48-well plate that was pre-coated with LM511 and contained neural differentiation media (neurobasal medium, NDM), supplemented with 1× B27, 1× N2, and 10 ng/ml BDNF (Invitrogen, Carlsbad, CA). NDM was changed every 3 days. Immunostaining was performed on day 10 (d10). Neurospheres were fixed using 4% paraformaldehyde for 15 min and then treated with 0.1% TritonX-100 for 30 min. After incubating with 1% BSA-PBS for 30 min at RT, cells were treated with primary antibodies [mouse anti-microtubule-associated protein 2 (MAP2; 1:200 dilution; Sigma–Aldrich)] overnight at 4°C. After washing with PBS, the cells were incubated with secondary antibodies (Alexa Fluor 488 donkey anti-mouse IgG; 1:1,000 dilution) for 1 h at RT. Following this, the cells were treated with 2 µg/ml Hoechst 33342 solution for 15 min at RT. Neurite length per cell and nuclei number were analyzed and calculated using an InCell analyzer 1000 (GE Healthcare, Tokyo, Japan). Images

were obtained using a 10x objective; furthermore, 9 images were acquired for each well. Sphere area and neurite migrations were investigated using Image J.

### 3.2.5 Microarray and bioinformatics analysis

On day 2 (d2), neurospheres for microarray were treated with PAMAM dendrimer-NH<sub>2</sub> (0.3 µg/ml) for 72 h. Four neurospheres from different experimental groups were pooled together separately. RNAs were isolated from each group at day 5. To detect changes in gene expression in neurospheres after PAMAM dendrimer exposure, microarray analyses were performed on two RNAs samples using a microarray (Sureprint G3 Human GE 8 × 60K Ver.2.0 1color 4; Agilent Technologies Inc., Santa Clara, CA, USA). The arrays were hybridized and scanned in accordance with the manufacturer's directions at the facility of Hokkaido System Science Co., Ltd. (Sapporo, Japan). The raw data were normalized and filtered by expression to the cut-off low values and then filtered by flag tag to remove entities that were not detected using GeneSpring GX12.10 software (Agilent Technologies). The microarray data were submitted to Gene Expression Omnibus (GEO) and registered as GSE65875 (<http://www.ncbi.nlm.nih.gov/geo/query/acc.cgi?acc=gse65875>). Genes with fold changes in log<sub>2</sub> expression values of >1.5 or ≤1.5 from each group were selected and combined to generate a common entity list. 32 Genes from the commonly responsive list were analyzed using Single Experiment Analysis (SEA) of GeneSpring to find matching genes in the WikiPathways. Matched gene entities from the top five pathways were selected; these 12 genes were then analyzed using the

natural language processing (NLP) network analyses of GeneSpring to identify extend interactions.

### 3.2.6 Quantitative gene expression analysis

In order to confirm gene expression, On day 2 (d2), neurospheres for RT-PCR were treated with PAMAM dendrimer-NH<sub>2</sub> (0.3 µg/ml, 1 µg/ml 3 µg/ml) for 72 h. RNAs were isolated from each group at day 5. RNAs was extracted and purified using the RNeasy Micro kit (Qiagen, Hilden, Germany) according to the manufacturer's protocol. The RNA quality and quantity were then examined using 2100 Bioanalyzer (Agilent Technologies, Santa Clara, CA, USA). High-Capacity RNA-to-cDNA kit (Applied Biosystems, Foster, California, USA) was used for RNA reverse transcription. Power SYBR green PCR master mix (Applied Biosystems, Foster, California, USA) and a MicroAmp Optical 96-Well Reaction Plate were used for real-time PCR with the 7000 Sequence Detection System (ABI PRISM, Foster City, USA). The following primer sets were used: TFPI2, 5'-TTCAGACTGAGGCTTCTATGGG-3' (forward) and 5'-GTAAAACGACGGCCAGTTGAAGATACAGCTACCGTCTACTGC-3' (reverse); Spry1, 5'-GTAAAACGACGGCCAGTGCGGTTTAGGCAATTTGTGATT-3' (forward) and 5'-CCCTGGCATTACTTGGGAGT-3' (reverse); EGR2, 5'-AGCTTTGCTCCCGTCTCTG-3' (forward) and 5'-AGCTGGCACCAGGGTACT-3' (reverse); IGFBP3, 5'-AGAGCACAGATACCCAGAACT-3' (forward) and 5'-TGAGGAACTTCAGGTGATTCAGT-3' (reverse); ADM,

5'-ACTTCGGAGTTTTGCCATTG-3' (forward) and  
5'-CTCTTCCCACGACTCAGAGC-3' (reverse); KCNJ2,  
5'-TGTTTTCCAAAGCAGAAGCA-3' (forward) and  
5'-CCCATCTTGACCAGTACCGT-3' (reverse);

### 3.2.7 Statistical analysis

Quantitative data were expressed as the percentage of the control  $\pm$  SD of at least three independent experiments. Analyses were performed using SPSS statistics v.19 (IBM, Tokyo, Japan). Statistical significance was determined by one-way ANOVA, followed by the Dunnett's tests for pairwise comparisons. Differences were considered statistically significant when  $P < 0.05$ .

## 3.3 Results

### 3.3.1 Neurosphere assay for assessing test chemicals

This culture system was established in last section, for neurosphere formation, neurospheres were cultured in uncoated round bottom plate from day 0 to day 2 (Fig. 3-1C). Human progenitor cells formed spheres during 3-D cell culture, and exposure to PAMAM dendrimers was conducted for 3 days after sphere formation from day 2 to day 5. After transfer to the NDM media, spheres grew and neurite cells migrated. After plating for adhesion, polarized individual cells migrated outward from the spherical center after 24 h. At day 5, the cell body size and projection length increased (Fig. 3-1D); at 10 days, cellular projections increased not only in size but also in

density (Fig. 3-1E). Individual cells displayed multiple neurite outgrowths and dendritic spines, which are typical characteristics of both immature and mature neuronal phenotype (Fig. 3-1F).

### 3.3.2 Incorporation of PAMAM dendrimers in neurospheres

To examine the bioincorporation of PAMAM dendrimers in neurospheres, Alexa-PAMAM conjugates were incubated with neurospheres for 3 days. Alexa 488-conjugates was used in sphere assay, but not the Alexa546 for intra-sphere distribution because fluorescent activity of Alexa 488 is weaker than it of Alexa. It was hard to get clear picture for Alexa 488 distributions because sphere is thickness. To confirm that free fluorescent agent are not able to uptake in neurospheres, a group of neurospheres were treated with PAMAM dendrimers for 3 days and then treated for 72 h with the fluorescent agent only. No fluorescent signal was observed in the neurospheres. For Alexa-PAMAM conjugate-treated group, Alexa-PAMAM conjugate was incubated with neurospheres at day 2 (d2). Cross-section images of neurospheres were shown in Fig. 3-2A, B and C. The 3-D images were generated using cross-section images and 3-D images were reversed to show the center of neurospheres. (Fig. 3-2D, E, F). The Alexa-546 fluorescence signal was only observed on the surface of neurospheres at day 3 (Fig. 3-2A, D), and an increasing number of Alexa-PAMAM conjugates was observed within the neurospheres at day4 (Fig. 3-2B, E) and day 5 (Fig. 3-2 C, F). The results showed a time dependent bio distribution of PAMAM dendrimer and serve as evidence that Alexa-PAMAM was located in the

center of neurospheres after 3 days of exposure.

### 3.3.3 Effect of PAMAM dendrimers on proliferation and migration of neurospheres

To study the effect of PAMAM dendrimers on proliferation, newly synthesized DNA of hNPCs was labeled with a bright fluorescently (EdU), nuclei was labeled with Hoechst 33342. The typical images (4×) of PAMAM dendrimers are shown in Figure 3-3(A–L). To quantify the effects of the dendrimers, neurosphere area was measured using Image J. The mean area of the neurosphere area decreased comparison with that observed in the controls (Fig. 3-4). Proliferation of cells in the flare areas which is shifted from the neurosphere core was investigated. These cells were considered as newly generated cells after PAMAM exposure. The EdU positive cell number decreased in flare area, suggest that PAMAM dendrimer inhibit migration but also cell proliferation.

### 3.3.4 Effect of PAMAM dendrimers on neuronal differentiation of neurospheres

To study the developmental neurotoxicity of PAMAM dendrimers, the neurite of neurospheres were immunohistochemically stained with anti-MAP2 protein antibody on day 10. The typical effects of PAMAM dendrimers are shown in Figure 3-5 (A–I). To quantify the effects of the dendrimers, the central core sizes of the neurosphere without flare areas and the flare areas that indicated cell migrations and cell proliferations were measured using Image J software. PAMAM dendrimer-NH<sub>2</sub> dose-dependently and significantly inhibited cell migration and cell proliferation, the mean area of the extended neuron decreased comparison with that observed in the

controls (Fig. 3-6). Alexa-PAMAM conjugates at a concentration of 10  $\mu\text{g/ml}$  inhibited cell migration; the extent of inhibition was similar to that observed using PAMAM-NH<sub>2</sub> dendrimers (Fig. 3-5I); however, Alexa-PAMAM conjugates did not affect migration or differentiation, whereas PAMAM-NH<sub>2</sub> dendrimers did at a concentration of 1  $\mu\text{g/ml}$  (Fig. 3-5H), suggest that surface group (NH<sub>2</sub>) is important to understand PAMAM toxicity. PAMAM-SC did not exert similar effects on MAP2-positive neurospheres at any test concentration (Fig. 3-5E, F).

The effects of PAMAM dendrimers on neurite length per cell and nuclei number that migrated from neural spheres were investigated (Fig. 3-7) and quantitatively determined. However, the dendrimers did not inhibit neurite length per cell at any concentration tested in the present study. In contrast, neurite length per cell significantly increased at concentration of 10  $\mu\text{g/ml}$  (Fig. 3-8A), and this may be because of small cell density lead to long neurite length, a decreased number of live cells was observed after PAMAM- NH<sub>2</sub> exposure. (Fig. 3-8B).

### 3.3.5 Gene expression profiling in PAMAM dendrimer-exposed spheres by microarray analyses and RT-PCR

The expression of 50,739 genes was detected by microarray analysis after PAMAM dendrimer exposure. Genes those are not detected and with low expression value were filtered, leaving behind 25,622 genes. With fold changes in log<sub>2</sub> expression values of  $>1.5$  or  $\leq 1.5$ , 289 and 171 of the entities were filtered from two independent experiments, respectively. Thirty-two of these genes were responsive in both

experiments.. These 32 genes were then analyzed by SEA to find matching genes in WikiPathways. Pathway analysis showed that direct interactions, Network targets and regulators pathway, and Hs\_Adipogenesis were the most matched pathways (Table 1). The matched gene expressions are shown in Table 2. Most of the matched genes, except *CYP26A1*, were down regulated. It was then analyzed how the genes interact with each other in natural language processing method. The result revealed three independent networks. Early growth response gene 1 (*EGRI*) (Fig. 3-9A), insulin-like growth factor-binding protein 3 (*IGFBP3*) (Fig. 3-9B), tissue factor pathway inhibitor (*TFPI2*), and adrenomedullin (*ADM*) (Fig. 3-9C) were the key node in each network. Therefore, the expression of key genes (*TFPI*, *SPRY2*, *IGFBP3*, *KCNJ2*, *ADM* and *EGRI*) were then confirmed using RT-PCR (Fig. 3-10). All selected genes were down regulated from concentration 1 µg/ml except *EGRI*.

### 3.4 Discussion and Summary

In order to define the migration and differentiation on human during nervous development after intracerebroventricular injection of PAMAM dendrimer, a hNPCs based neurosphere system was performed. To the best of my knowledge, this is the first study to profile the gene response of neurospheres to PAMAM dendrimer exposure using microarray analysis. This showed the mechanism of cationic PAMAM dendrimers-NH<sub>2</sub> affect neurosphere.

A few studies have reported the effects following exposure to PAMAM

dendrimers. For example, an *in vitro* study suggested that PAMAM induced the aggregation of human platelets in plasma [60]. It has recently been suggested that the exposure of PAMAM dendrimers to animals induces surface chemistry-dependent central neural cytotoxicity, whereas penetration into living neurons was observed after intraparenchymal or intraventricular injection of these molecular complexes [61]. In my previous study, using monolayer culture assay, G4 PAMAM-NH<sub>2</sub> did not inhibited cell proliferation at 1ug/ml. However, using neurospheres culture system in this part, G4 PAMAM-NH<sub>2</sub> significantly inhibited cell proliferation at 1ug/ml. suggested that neurosphere culturesystem is sensitive compare with 2-D monolayer culture system.

In the present study, hNPCs was used to study the effects of G4 PAMAM dendrimers on neuronal differentiation. hNPCs were exposed to various concentrations of dendrimers for 72 h and then allowed to differentiate for additional 5 days. A surface type-dependent toxicity was observed. Cationic NH<sub>2</sub> but not anionic SC surface functional group dendrimers induced migration but not differentiation of neurospheres. Dendrimers were observed in neurospheres after 2 days of exposure, indicating that PAMAM dendrimer nanoparticles can penetrate into neurospheres through superficial cells. *TFPI2*, *IGFBP3*, and *EGR1* were commonly responsive among specific pathways and show as key nodes in network analysis, suggesting that the restrained expression of *TFPI2*, *IGFBP3*, and *EGR1* plays a very important role after exposure to PAMAM dendrimers and that these genes may be related to cell migration during neurodevelopment of neurospheres.

It is important to understand the drug delivery system of dendrimers in the human body. The biodistribution of PAMAM dendrimers has been studied in mice and rabbits. The present study simulated human tissue development using a 3-D culture system to study the biodistribution of dendrimers, using dendrimer-Alexa conjugates to track PAMAM dendrimers after exposure to neurospheres. PAMAM dendrimers were only observed on the surface of neurospheres during the initial 24 h of exposure; however, conjugates were observed in neurospheres after 2 days of exposure. These findings indicate that PAMAM dendrimer nanoparticles can penetrate into neurospheres through superficial cells.

Neurospheres were allowed to differentiate for additional 5 days in NDM and neurite extension and differentiation was studied because they play a very important role during neurodevelopment. PAMAM-SC did not affect neurospheres at any test concentration. PAMAM-NH<sub>2</sub> significantly inhibited neurosphere flare areas which indicate as cell migration and perforation at concentrations of 1 µg/ml, 3 µg/ml and 10 µg/ml. PAMAM-NH<sub>2</sub> did not inhibit neurite length per cell at any concentration tested in the present study. In contrast, neurite length per cell significantly increased at a concentration of 10 µg/ml, and this may be because of the PAMAM-induced decrease in the number of live cells. Cell proliferation assay was performed respectively using NEM after PAMAM exposure. Neurosphere proliferation and migration was inhibited for PAMAM-NH<sub>2</sub> at concentrations of 1 µg/ml, 3 µg/ml and 10 µg/ml. To confirm the inhibitory effect on cell proliferation, high magnification images (10x) were acquired.

Proliferation of cells in the flare areas which is shifted from the neurosphere core was investigated. The EdU positive cells significantly decreased in flare area, suggest that PAMAM dendrimer inhibit migration but also cell proliferation at concentration of 1µg/ml. These results suggested that PAMAM may inhibited cell viability through proliferation and cell migration. However, after PAMAM exposure on neurosphere, no persistent effect on neurite extension of neurosphere, suggested that PAMAM dendrimer do not have specific development neurotoxicity.

Microarray analysis after PAMAM exposure showed a down regulation of *EGR1*, which plays an important role in regulating cell proliferation and differentiation. Overexpression of *EGR1* can induce the osteogenic differentiation of dental stem cells by regulating the expression of *DLX3* and *BMP2*. Egr1 is one of the key transcription factors in extremely low-frequency electromagnetic field (ELF-EMF)-induced neuronal differentiation. The observed down regulation of *EGR1* in the present study may be due to the positive charge of PAMAM dendrimer-NH<sub>2</sub>, which may influence ELF-EMF and induce neuronal migrations. *SPRY1* may contribute to congenital disorders involving tissues of neural crest origin. Down regulation of *SPRY1* revealed that PAMAM dendrimer exposure during fetal brain development may lead to congenital disorders. Overexpression of *CYP26A1* induces neurodegenerative diseases by the enhancement of retinoic acid (RA) metabolites. Cationic PAMAM induces the overexpression of *CYP26A1*, which is considered as a potential risk for inducing some neural toxicity in the human brain. The observed down regulation of genes mostly

related to direct interactions and network targets and regulators pathways has revealed that PAMAM dendrimers affect regulator function through a direct interaction. Genes with similar functions usually fall into the same functional modules. The revealed genes were checked whether they are connected with each other using a bioinformatics approach. *EGR1*, *TFPI2*, *IGFBP3*, and *ADM* were found to be the key node in their respective networks. The expressions of these genes were then checked by RT-PCR, most of the genes were down regulated. It was suggested that the positive charge of PAMAM dendrimer-NH<sub>2</sub> may influence ELF-EMF and inhibit neuronal proliferation, lead to congenital disorders.

In conclusion, exposure of neurosphere to 1, 3, or 10 µg/ml concentrations of PAMAM dendrimers resulted in a reduced number of MAP2-positive cells but not neurite length/cells, indicating an inhibitory effect on neuronal migration but not differentiation. PAMAM dendrimer nanoparticles can penetrate into neurospheres through superficial cells. Microarray gene pathway analyses revealed a regulation of various genes for G4-PAMAM dendrimers, these genes are involved in various signal transduction pathways, and direct interactions and network pathways are the most related. Network analysis using the bioinformatics approach revealed that *TFPI2*, *IGFBP3*, and *EGR1* play a very important role after exposure to PAMAM dendrimers. These findings suggest that the exposure of pre-differentiated cells to PAMAM dendrimers results in a change in cell migrations through *TFPI2*, *IGFBP3*, and *EGR1* regulated pathways. The biodistribution and DNT of PAMAM dendrimer was

assessed, use of PAMAM-NH<sub>2</sub> as drug carrier may induce adverse reactions on neurons.

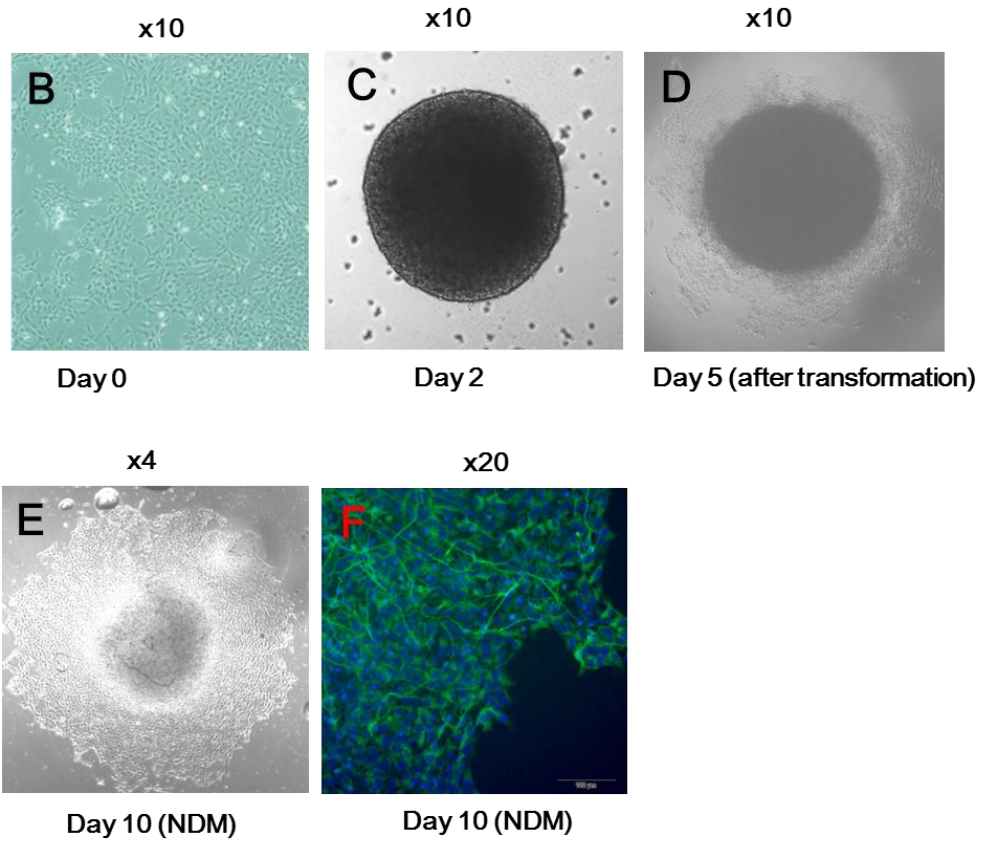
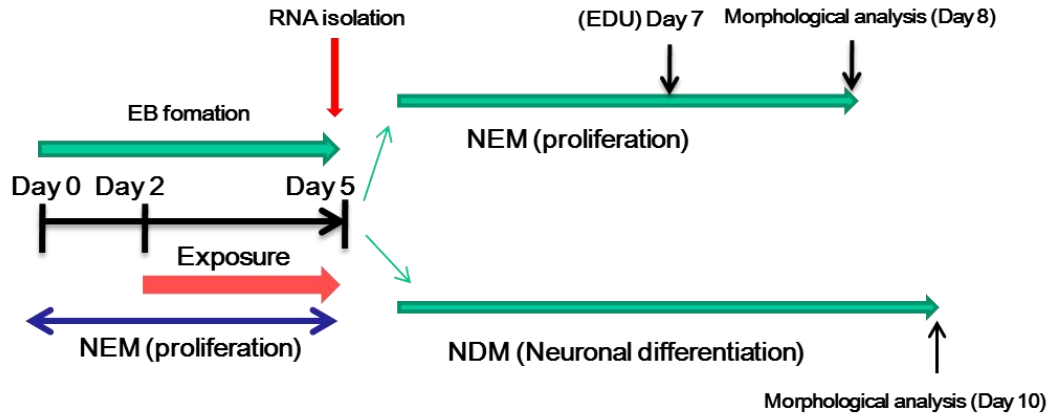


**Fig. 3-1** Experimental time schedules of PAMAM exposure, proliferation and differentiation (A). Gene expression analysis was conducted using total RNAs from neurospheres on day 5, followed by proliferation assay on day 5 to day 8. Morphological photographs for proliferation and differentiation of hNPCs in the neurosphere assay (B–F).

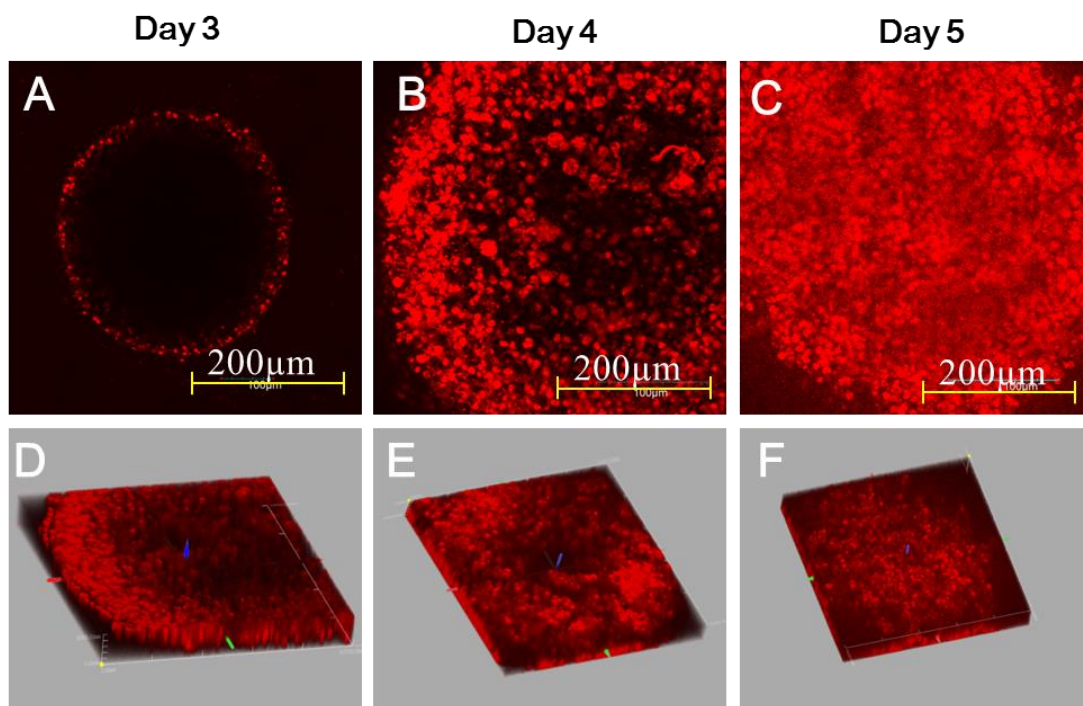


**Fig. 3-2** Distribution images of PAMAM-NH<sub>2</sub> dendrimers using a confocal laser microscope. 2-D photographs of sphere cross section (A, B, C) and 3-D images (D, E, F) were acquired at day 3 (A, D), day 4 (B, E) and day 5 (C, F) time points after starting the sphere formation. 3-D images (D, E, F) were located from the top of sphere to center, they were reversed images and their thickness were 30 μm.

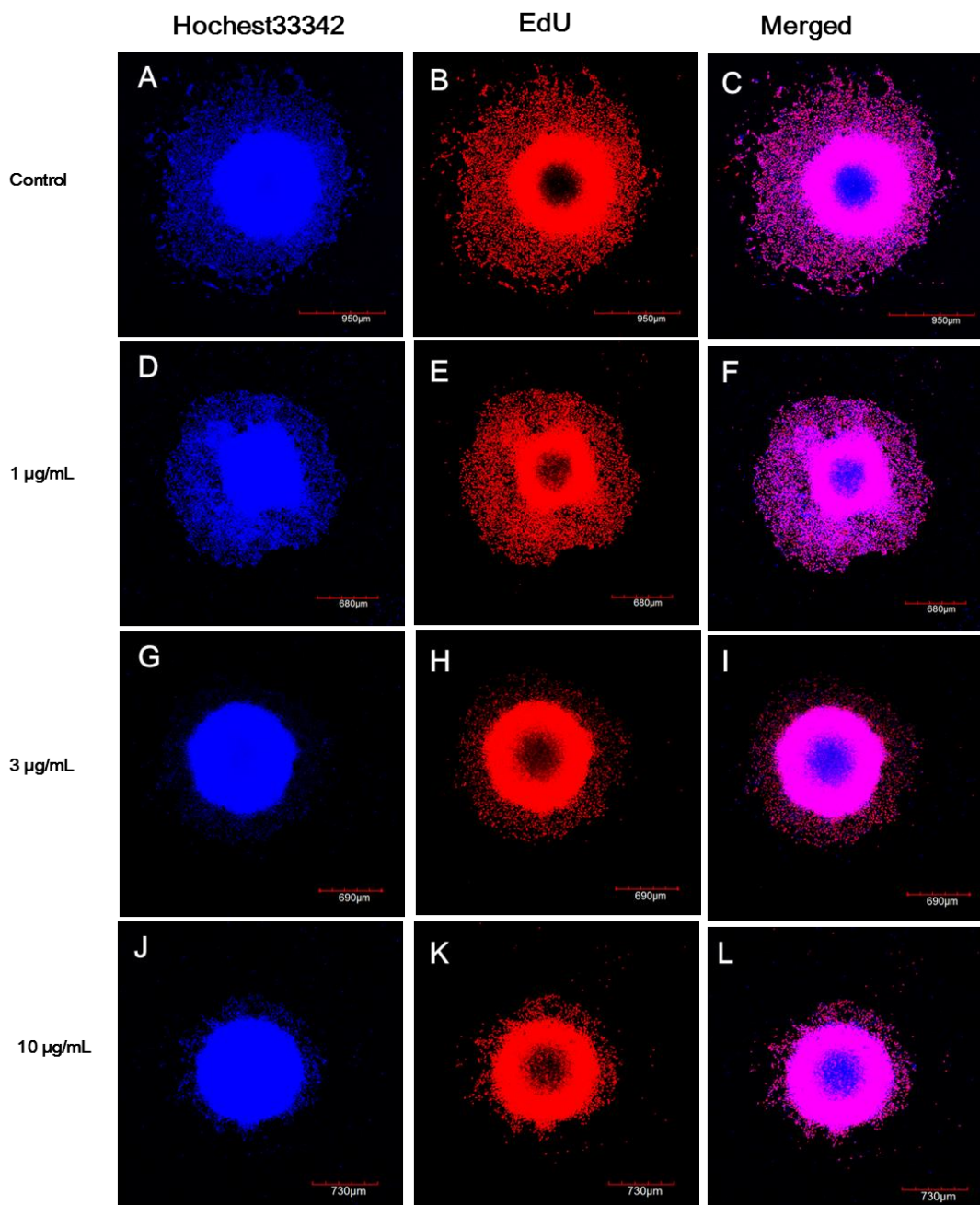


**Fig. 3-3** Effects of PAMAM dendrimer on migration and proliferation of neurosphere. Representative images were acquired at day 8 PAMAM-NH<sub>2</sub> treatment at concentrations of 1, 3 or 10 µg/ml for 72 h. Nuclei were stained with Hoechst 33342 (A,D,G,J), newly generated cells from day 7 to day 8 was labeled by EDU (Alexa 555 fluorescence) (B,E,H,K).

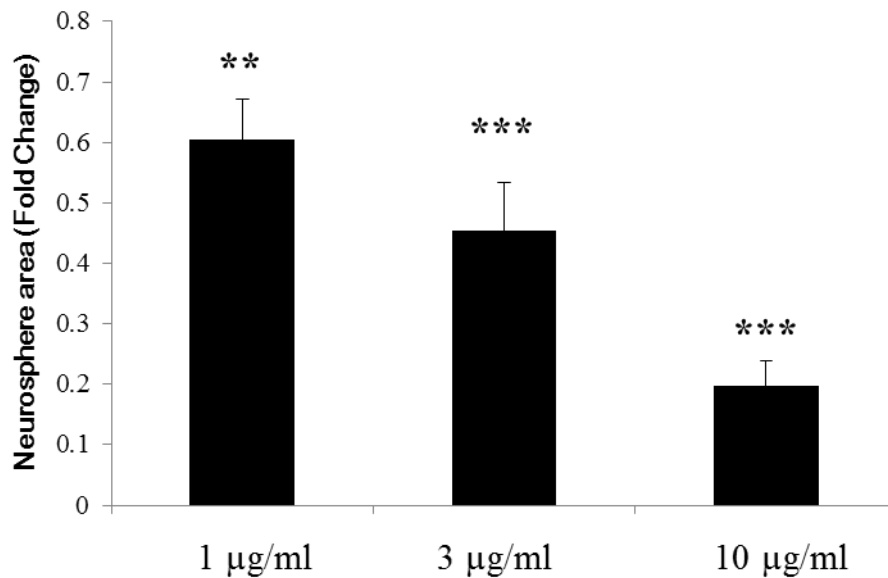


**Fig. 3-4** Quantified data on the effects on proliferation and migration of PAMAM-NH<sub>2</sub> were acquired using Image J for measurement of sphere area. Data are expressed as the percentage of the control  $\pm$  SD for four independent experiments. \*  $P < 0.05$ , \*\* $P < 0.01$ , and \*\*\* $P < 0.001$  were considered to be statistically significant differences between the treatment group and the vehicle control.

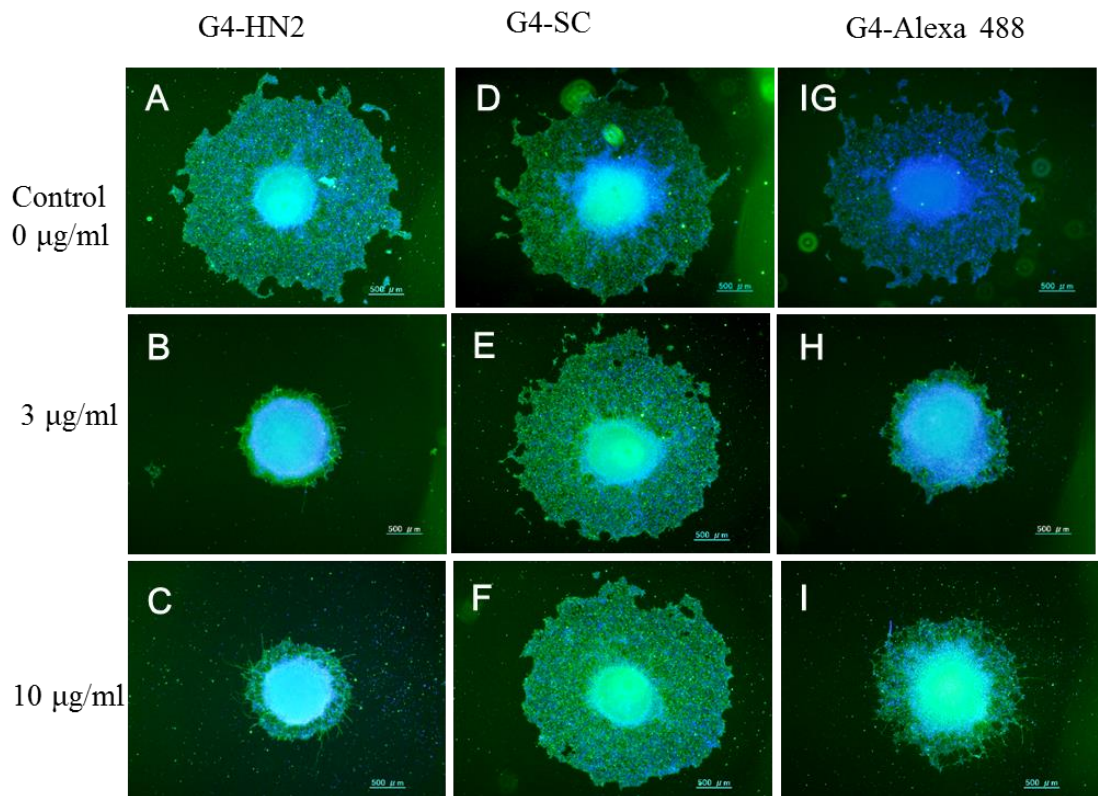


**Fig. 3-5** Effects of PAMAM dendrimer on migration and differentiation of neurosphere. Representative images were acquired without PAMAM treatment (vehicle control) or after 72 h of PAMAM G4-NH<sub>2</sub> (A-C), PAMAM-SC (D-F) or Alexa488-labeled PAMAM-NH<sub>2</sub> (G-I) treatment at concentrations of 3 or 10  $\mu\text{g/ml}$ .

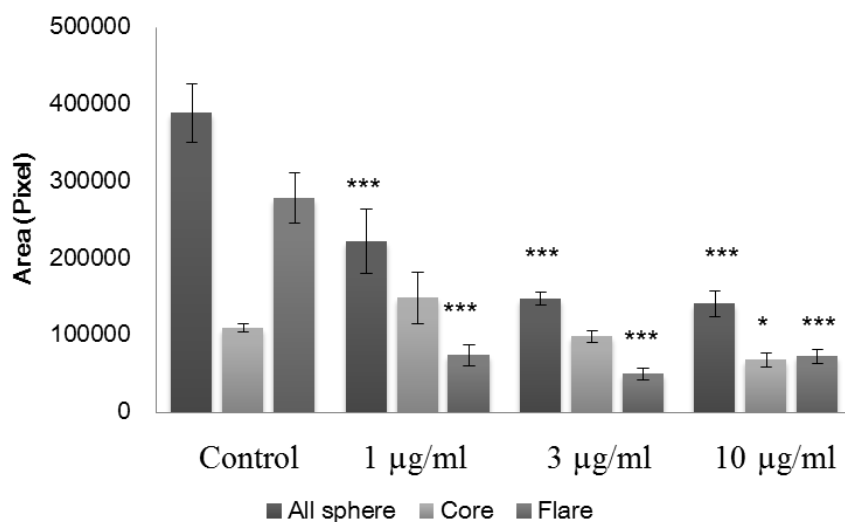


**Fig. 3-6** Quantified data on the effects on migration of PAMAM-NH<sub>2</sub> were acquired using Image J ver4 for measurement of sphere area and flare area. Data are expressed as the percentage of the control  $\pm$  SD for four independent experiments. \*  $P < 0.05$ , \*\* $P < 0.01$ , and \*\*\* $P < 0.001$  were considered to be statistically significant differences between the treatment group and the vehicle control.

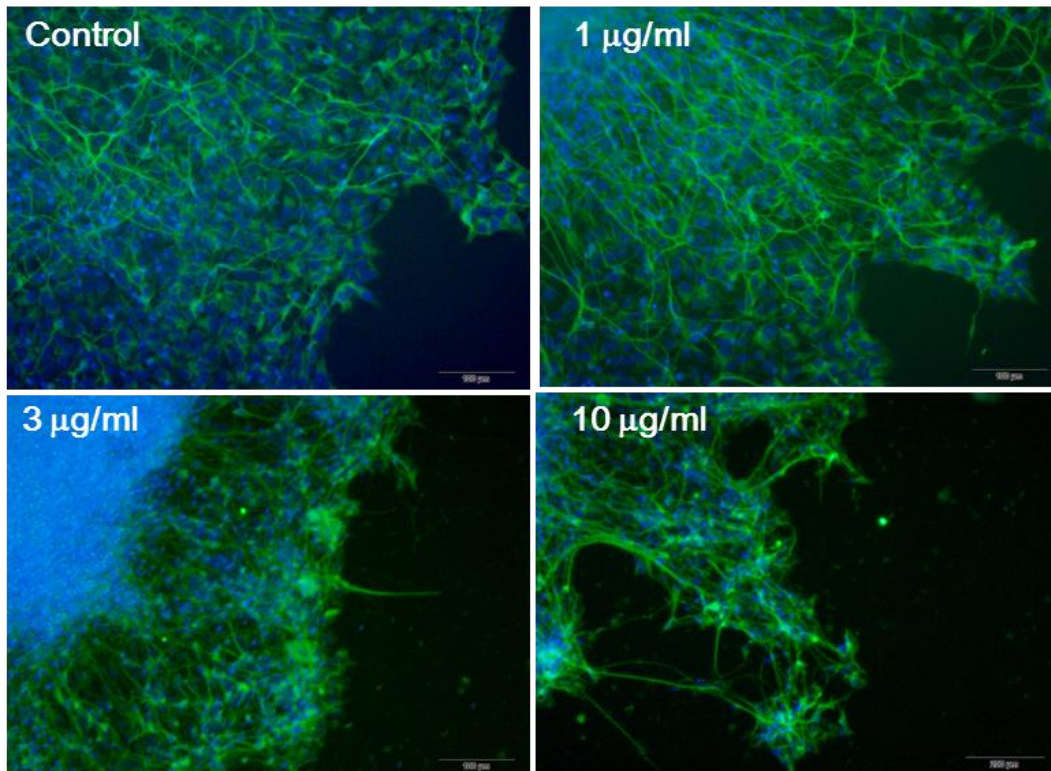


**Fig. 3-7** Photographs and quantified data of neurite length and nuclei number after PAMAM-NH<sub>2</sub> treatment were measured using the In cell analyzer 1000. Morphology of neuronal cells at the 10x magnification of optical lens was acquired.

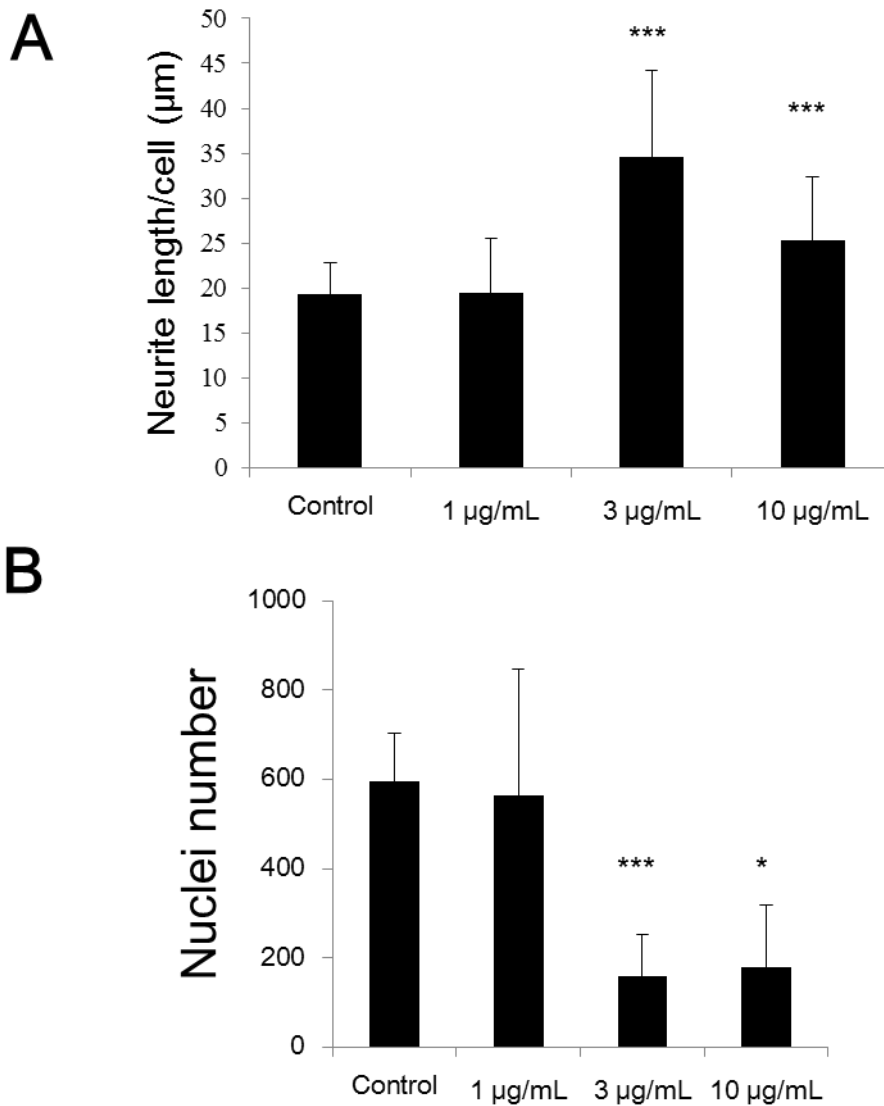


**Fig. 3-8** Neurite lengths (A) and nuclei number (B) were measured. Data are expressed as the percentage of the control  $\pm$  SD for three independent experiments. \* $P < 0.05$ , \*\* $P < 0.01$ , and \*\*\* $P < 0.001$  were considered to be statistically significant differences between the treatment group and the vehicle control.

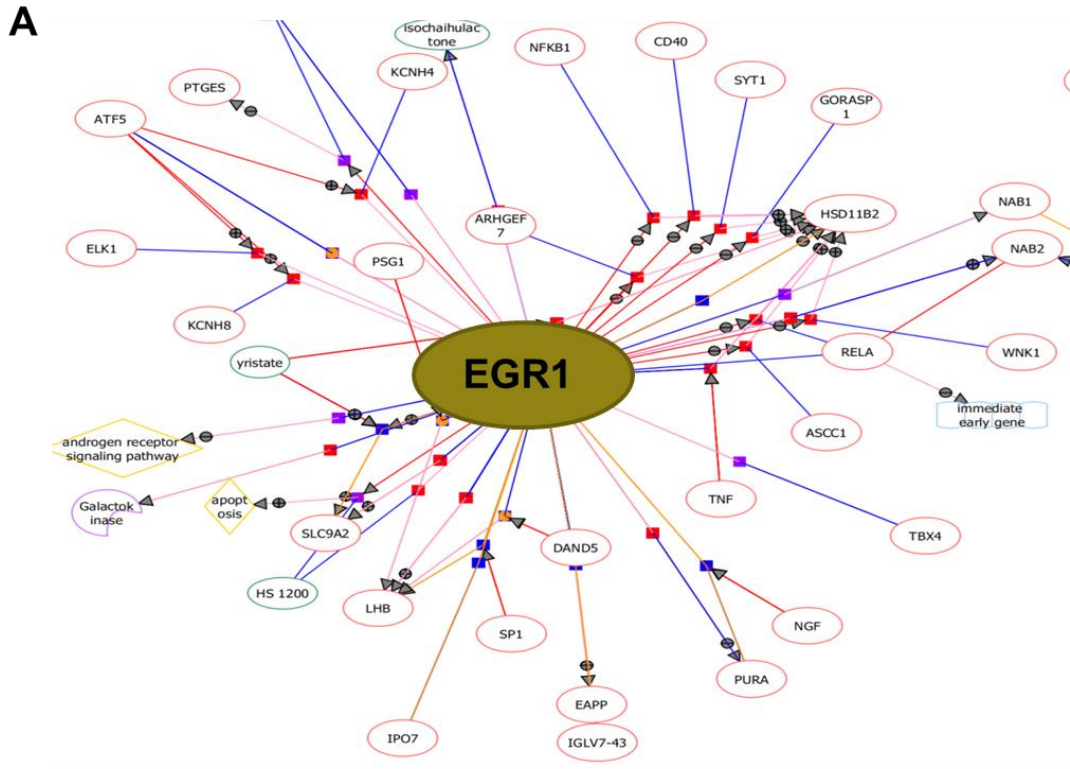


**Fig. 3-9** Network analysis of genes with more than 1.5-fold changes selected from microarray analysis. Matched gene entities from the top five pathways as shown in Table 2 were then analyzed using natural language processing (NLP) network analyses from GeneSpring to find expanded interactions for *EGR1* (A).

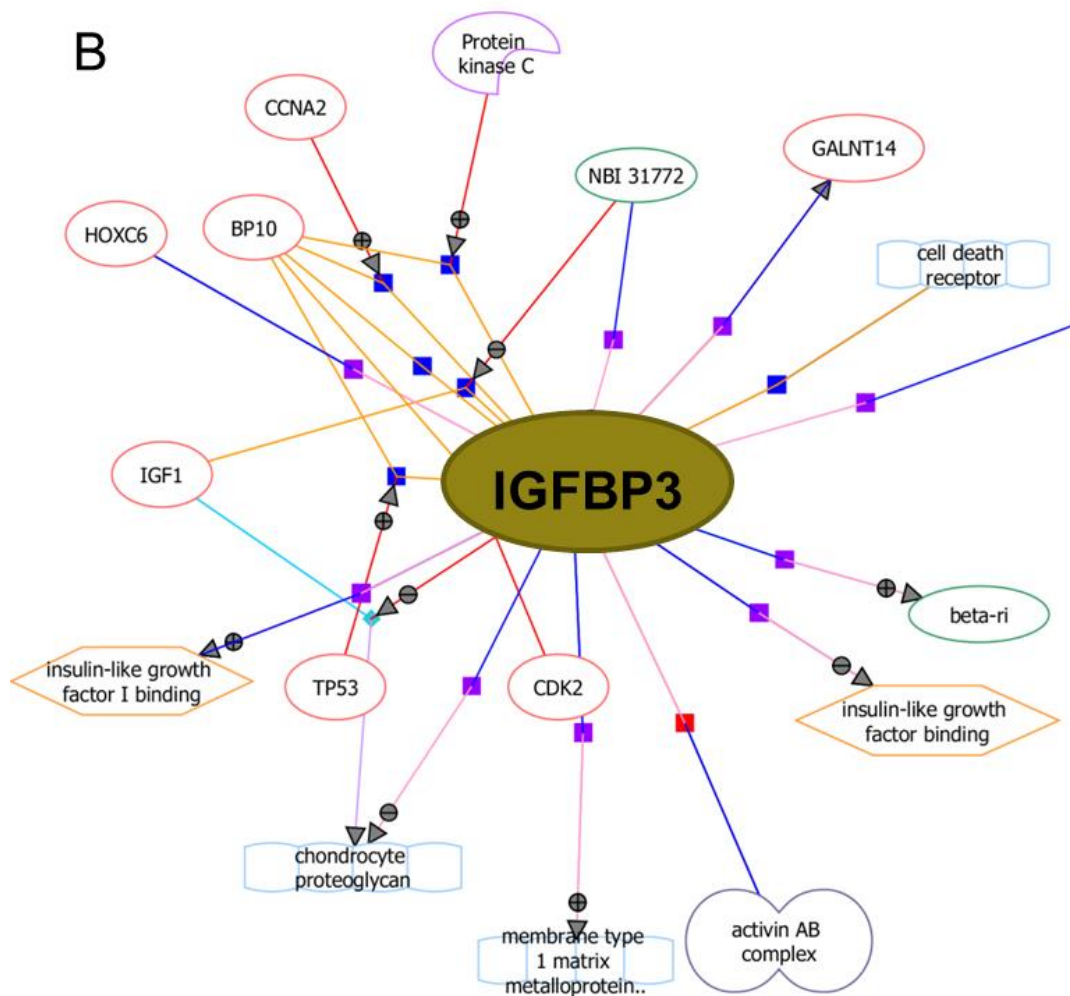


**Fig. 3-9** Analyzed using natural language processing (NLP) network analyses from GeneSpring to find expanded interactions for *GFBP3* (B).

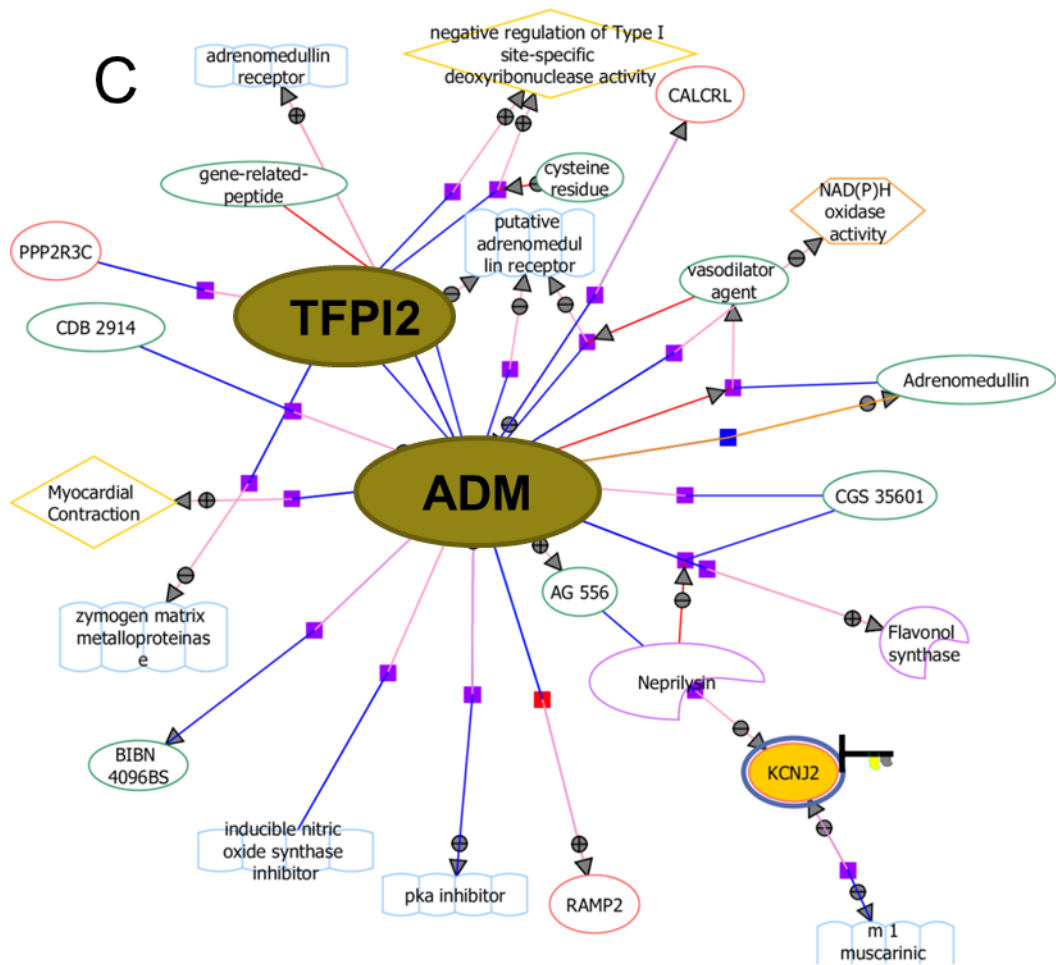


**Fig. 3-9** Analyzed using natural language processing (NLP) network analyses from GeneSpring to find expanded interactions for *TFPI2* and *ADM* (C).

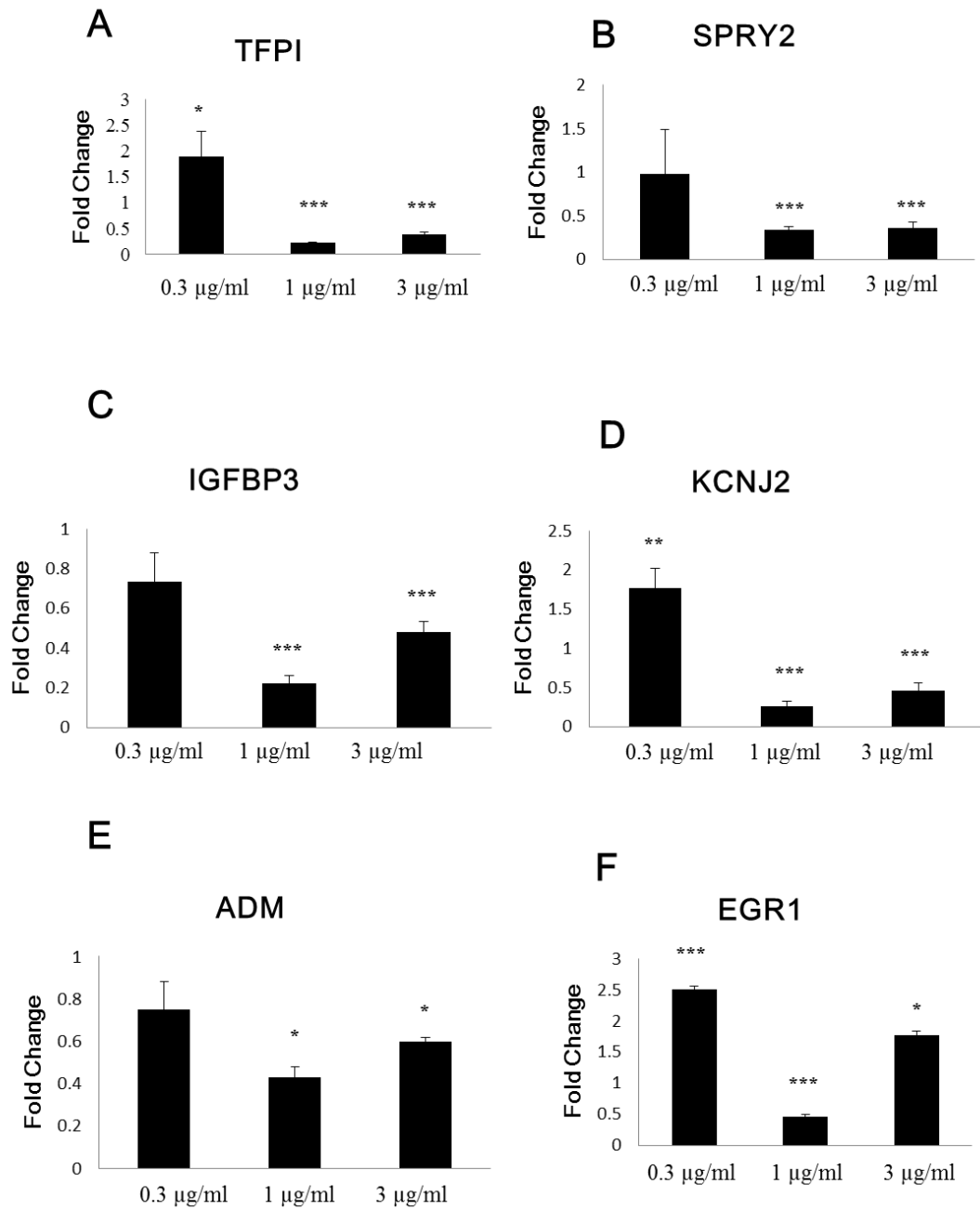


**Fig. 3-10** Expression of selected genes was analyzed by RT-PCR. Results of PAMAM treatment groups were related to controls set to one. \*  $P < 0.05$ , \*\*  $P < 0.01$ , and \*\*\*  $P < 0.001$  were considered to be statistically significant differences between the treatment group and the vehicle control.

**Table 3-1.** Functional annotation pathway listed by pathway analysis.

Functional annotated pathways	<i>P</i> -value	Matched gene entities	Gene entities in the pathway
Direct Interactions	4.1E-10	8	371
Network Targets and Regulators	1.7E-08	8	407
Hs_Adipogenesis_WP236_44941	0.0043	2	131
Hs_Myometrial_Relaxation_and_Contraction_Pathways_WP289_45373	0.0060	2	156
Hs_Regulation_of_Insulin-like_Growth_Factor_(IGF)_Activity_by_Insulin-like_Growth_Factor_Binding_Proteins_(IGFBPs)_WP1899_45051	0.0074	1	10

**Table 3-2.** Pathway analyses after PAMAM dendrimer exposure. Gene expression was shown as the log fold change referring to the control level. Genes which responses in repeated pathways were highlighted.

Direct Interactions		
Genes	Log2 FC in array1	Log2 FC in array 2
KCNJ2	-2.6087	-2.0524
TFPI2	-2.5823	-2.0296
EGR1	-2.5140	-2.5834
<b>FAM150B</b>	-1.7865	-1.2568
SPRY1	-1.4594	-1.7948
<b>PIP5K1B</b>	-1.4113	-1.5038
SPRY4	-1.3292	-0.6029
CDH6	-0.8651	-1.0540
Network Targets and Regulators		
Genes	Log2 FC in array 1	Log2 FC in array 2
KCNJ2	-2.6087	-2.0524
TFPI2	-2.5824	-2.0296
<b>FAM150B</b>	-1.7865	-1.2568
SPRY	-1.4594	-1.7948
<b>PIP5K1B</b>	-1.4113	-1.5038
SPRY4	-1.3292	-0.6029
CDH6	-0.8651	-1.0540
KCNJ2	-2.6087	-2.0524
Hs_Adipogenesis_WP236_44941		
Genes	Log2 FC in array 1	Log2 FC in array 2
CYP26A1	1.3427	1.5846
EGR2	-1.2301	-1.3729
Hs_Myometrial_Relaxation_and_Contraction_Pathways_WP289_45373		
Genes	Log2 FC in array 1	Log2 FC in array 2
ADM	-2.9762	-2.2459
IGFBP3	-2.7287	-2.1465
Hs_Regulation_of_Insulin-like_Growth_Factor_(IGF)_Activity_by_Insulin-like_Growth_Factor_Binding_Proteins_(IGFBPs)_WP1899_45051		
Genes	Log2 FC in array 1	Log2 FC in array 2
IGFBP3	-2.7287	-2.146

## Chapter 4 Conclusions and future research

### 4.1 Conclusions in chapter 2

In chapter 2, a DNT test system was established using hNPCs and it was found that:

1. Intact LM511 substrates are qualitatively important for efficient and stable hNPCs differentiation. The addition of poly-L-ornithine is advantageous for hNPCs proliferation, but not suitable for stable hNPCs differentiation.
2. Benzo[a]pyrene and 5-Azacytidine were applied to the established system. Both chemicals significantly inhibited cell migration and induced apoptosis.
3. The established LM511 culture system can distinguish between neurotoxic and non-neurotoxic substances, and it is suggested that this novel model is a good tool for investigations of environmental neurotoxicity.

### 4.2 Conclusions in chapter 3

It was then assessed the developmental neurotoxicity of PAMAM using the established system. It was identified that:

1. A reduced number of MAP2-positive cells but not neurite length/cells after G4-PAMAM-NH<sub>2</sub> dendrimers treatment, indicating an inhibitory effect on neuronal migration but not differentiation.
2. PAMAM-NH<sub>2</sub> dendrimer nanoparticles can penetrate into neurospheres through superficial cells on it.
3. Network analysis showed three connected networks of the selected gene targets in direct interactions, Network targets and regulators, adipogenesis, myometrial relaxation/contraction, and insulin-like growth factor signaling.
4. *Egr1*, *IGFBP3*, *TFPI2*, *ADM* were the key genes in each network, and the

expression of these genes was significantly downregulated.

5. The biodistribution and DNT of PAMAM dendrimer was fully assessed, use of PAMAM-NH<sub>2</sub> as drug carrier may induce adverse reactions on neurons.

### 4.3 Conclusions of this thesis

An efficient and stable culture system for DNT assessment was established using LM511 BM. Further, It was found that PAMAM-SC did not affect neurospheres at any test concentration. PAMAM-NH<sub>2</sub> can penetrate into neurospheres time dependently. Network analysis using the bioinformatics approach revealed that *TFPI2*, *IGFBP3*, and *EGR1* play a very important role after exposure to PAMAM dendrimers. Cell proliferation and cell migration was significantly inhibited at concentration of 3 µg/ml and 10 µg/ml. However, after PAMAM exposure on neurosphere, no persistent effect on neurite extension of neurosphere. These findings suggest that the exposure of neurosphere to PAMAM dendrimers results in a change in cell proliferation and cell migrations through *TFPI2*, *IGFBP3*, and *EGR1* regulated pathways. The biodistribution and DNT of PAMAM dendrimer was fully assessed, use of PAMAM-NH<sub>2</sub> as drug carrier may induce adverse reactions on neurons.

#### 4.4 Future work

1. The mechanism of PAMAM-NH<sub>2</sub> dendrimer induced developmental neurotoxicity will be studied. An enzyme activity assay and western blot analysis will be carry out to analysis PAMAM-NH<sub>2</sub> induced DNT. The cellular ROS needed to be detect after exposure.
2. The nontoxic PAMAM-SC should be assessed to find weather it can be used as drug carrier. A high concentration exposure assay and a gene expression profiling assay will be carried out to confirm the safety of PAMAM-SC.
3. Using the novel established culture system, neurotoxicity of other chemicals or nanoparticles will be assessed. DNT of PAMAM-NH<sub>2</sub> from generation 1 to generation 10 will be assessed using neurosphere.

## **Acknowledgments**

Though only my name appears on the cover of this dissertation, a great many people have contributed to its production. I owe my gratitude to all those people who have made this dissertation possible and because of whom my graduate experience has been one that I will cherish forever.

First and Foremost, I would like to express my sincere gratitude to Prof. Zhenya Zhang, Prof. Hideko Sone, Prof. YingnanYang, Prof. Motoo Utsumi, for their continuous support for my study and research.

I would further like to express my great appreciation to my thesis committee for their valuable and insightful comments, which helped me in improving this thesis. Special gratitude is expressed to Associate Prof. Zhongfang Lei for the encouragement and kind help during my Ph. D studies.

Last but not least, I would like to especially thank my parents. Words alone cannot express what I owe you for your encouragement and patient love, which enabled me to complete my study.

## References

- [1] Newkome G R, Childs B J, Rourke M J, Baker G R, Moorefield C N. Dendrimer construction and macromolecular property modification via combinatorial methods. *Biotechnol Bioeng*, 1998, 61(4): 243-253.
- [2] Bharatwaj B, Mohammad A K, Dimovski R, Cassio F L, Bazito R C, Conti D, Fu Q, Reineke J J, Da Rocha S R. Dendrimer nanocarriers for transport modulation across models of the pulmonary epithelium. *Mol Pharm*, 2014, 1(4): 43-153.
- [3] Khodadust R, Unsoy G, Gunduz U. Development of poly (i:C) modified doxorubicin loaded magnetic dendrimer nanoparticles for targeted combination therapy. *Biomedicine pharmacotherapie*, 2014, 68(8): 979-987.
- [4] Biswal B K, Kavitha M, Verma R S, Prasad E. Tumor cell imaging using the intrinsic emission from pamam dendrimer: A case study with hela cells. *Cytotechnology*, 2009, 61(1-2): 17-24.
- [5] Adeli M, Ashiri M, Chegeni B K, Sasanpour P. Tumor-targeted drug delivery systems based on supramolecular interactions between iron oxide-carbon nanotubes pamam-peg-pamam linear-dendritic copolymers. *J Iran Chem Soc*, 2013, 10(4): 701-708.
- [6] Zhu K, Guo C F, Lai H, Yang W L, Wang C S. Novel hyperbranched polyamidoamine nanoparticle based gene delivery: Transfection, cytotoxicity and in vitro evaluation. *Int J Pharmaceut*, 2012, 423(2): 378-383.
- [7] Wang P, Zhao X H, Wang Z Y, Meng M, Li X, Ning Q A. Generation 4 polyamidoamine dendrimers is a novel candidate of nano-carrier for gene delivery agents in breast cancer treatment. *Cancer Lett*, 2010, 298(1): 34-49.
- [8] Cui D M, Xu Q W, Gu S X, Shi J L, Che X M. Pamam-drug complex for delivering anticancer drug across blood-brain barrier in-vitro and in-vivo. *Afr J Pharm Pharmaco*, 2009, 3(5): 227-233.
- [9] Huang R Q, Qu Y H, Ke W L, Zhu J H, Pei Y Y, Jiang C. Efficient gene delivery targeted to the brain using a transferrin-conjugated polyethyleneglycol-modified polyamidoamine dendrimer. *Faseb J*, 2007, 21(4): 1117-1125.
- [10] Ke W L, Shao K, Huang R Q, Han L, Liu Y, Li J F, Kuang Y Y, Ye L Y, Lou J N, Jiang C. Gene

- delivery targeted to the brain using an angiopep-conjugated polyethyleneglycol-modified polyamidoamine dendrimer. *Biomaterials*, 2009, 30(36): 6976-6985.
- [11] Yan H H, Wang J Y, Yi P W, Lei H, Zhan C Y, Xie C, Feng L L, Qian J, Zhu J H, Lu W Y, Li C. Imaging brain tumor by dendrimer-based optical/paramagnetic nanoprobe across the blood-brain barrier. *Chem Commun*, 2011, 47(28): 8130-8132.
- [12] Mukherjee S P, Davoren M, Byrne H J. In vitro mammalian cytotoxicological study of pamam dendrimers - towards quantitative structure activity relationships. *Toxicol in Vitro*, 2010, 24(1): 169-177.
- [13] Bielawski K, Bielawska A, Muszynska A, Poplawska B, Czarnomysy R. Cytotoxic activity of g3 pamam-nh2 dendrimer-chlorambucil conjugate in human breast cancer cells. *Environ Toxicol Phar*, 2011, 32(3): 364-372.
- [14] Schleh C, Semmler-Behnke M, Lipka J, Wenk A, Hirn S, Schaffler M, Schmid G, Simon U, Kreyling W G. Size and surface charge of gold nanoparticles determine absorption across intestinal barriers and accumulation in secondary target organs after oral administration. *Nanotoxicology*, 2012, 6(1): 36-46.
- [15] Naha P C, Davoren M, Lyng F M, Byrne H J. Reactive oxygen species (ros) induced cytokine production and cytotoxicity of pamam dendrimers in j774a.1 cells. *Toxicol Appl Pharm*, 2010, 246(1-2): 91-99.
- [16] Hernando M D, Rosenkranz P, Ulaszewska M M, Fernandez-Cruz M L, Fernandez-Alba A R, Navas J M. In vitro dose-response effects of poly(amidoamine) dendrimers [amino-terminated and surface-modified with n-(2-hydroxydodecyl) groups] and quantitative determination by a liquid chromatography-hybrid quadrupole/time-of-flight mass spectrometry based method. *Anal Bioanal Chem*, 2012, 404(9): 2749-2763.
- [17] Ciolkowski M, Rozanek M, Szewczyk M, Klajnert B, Bryszewska M. The influence of pamam-oh dendrimers on the activity of human erythrocytes atpases. *Bba-Biomembranes*, 2011, 1808(11): 2714-2723.
- [18] Mukherjee S P, Lyng F M, Garcia A, Davoren M, Byrne H J. Mechanistic studies of in vitro cytotoxicity of poly(amidoamine) dendrimers in mammalian cells. *Toxicol Appl Pharm*, 2010,

248(3): 259-268.

- [19] Maher M A, Naha P C, Mukherjee S P, Byrne H J. Numerical simulations of in vitro nanoparticle toxicity - the case of poly(amido amine) dendrimers. *Toxicol in Vitro*, 2014, 28(8): 1449-1460.
- [20] Harry G J, Hooth M J, Vallant M, Behl M, Travlos G S, Howard J L, Price C J, McBride S, Mervis R, Mouton P R. Developmental neurotoxicity of 3,3',4,4'-tetrachloroazobenzene with thyroxine deficit: Sensitivity of glia and dentate granule neurons in the absence of behavioral changes. *Toxics*, 2014, 2(3): 496-532.
- [21] Myers G J, Davidson P W, Watson G E, Van Wijngaarden E, Thurston S W, Strain J J, Shamlaye C F, Bovet P. Methylmercury exposure and developmental neurotoxicity. *Bulletin of the World Health Organization*, 2015, 93(2): 1-32.
- [22] Orza A I, Mihiu C, Soritau O, Diudea M, Florea A, Matei H, Balici S, Mudalige T, Kanarpardy G K, Biris A S. Multistructural biomimetic substrates for controlled cellular differentiation. *Nanotechnology*, 2014, 25(6): 065-102.
- [23] Orza A, Soritau O, Olenic L, Diudea M, Florea A, Rus Ciuca D, Mihiu C, Casciano D, Biris A S. Electrically conductive gold-coated collagen nanofibers for placental-derived mesenchymal stem cells enhanced differentiation and proliferation. *Acs Nano*, 2011, 5(6): 4490-4503.
- [24] Hill E J, Woehrling E K, Prince M, Coleman M D. Differentiating human nt2/d1 neurospheres as a versatile in vitro 3d model system for developmental neurotoxicity testing. *Toxicology*, 2008, 249(2-3): 243-250.
- [25] Schulpen S H, Pennings J L, Piersma A H. Gene expression regulation and pathway analysis after valproic acid and carbamazepine exposure in a human embryonic stem cell based neuro-developmental toxicity assay. *Toxicol Sci*, 2015, 9(5): 33-50.
- [26] Schulpen S H, De Jong E, De La Fonteyne L J, De Klerk A, Piersma A H. Distinct gene expression responses of two anticonvulsant drugs in a novel human embryonic stem cell based neural differentiation assay protocol. *Toxicol in Vitro*, 2015, 29(3): 449-457.
- [27] Baumann J, Barenys M, Gassmann K, Fritsche E. Comparative human and rat "neurosphere assay" for developmental neurotoxicity testing. *Curr Protoc Toxicol*, 2014, 59 (1): 11-12.
- [28] Cossetti C, Alfaro-Cervello C, Donega M, Tyzack G, Pluchino S. New perspectives of tissue

- remodelling with neural stem and progenitor cell-based therapies. *Cell Tissue Res*, 2012, 349(1): 321-329.
- [29] Ryu J K, Cho T, Wang Y T, McLarnon J G. Neural progenitor cells attenuate inflammatory reactivity and neuronal loss in an animal model of inflamed ad brain. *J Neuroinflamm*, 2009, 6: 121-139.
- [30] Breier J M, Radio N M, Mundy W R, Shafer T J. Development of a high-throughput screening assay for chemical effects on proliferation and viability of immortalized human neural progenitor cells. *Toxicol Sci*, 2008, 105(1): 119-133.
- [31] Breier J M, Gassmann K, Kayser R, Stegeman H, De Groot D, Fritsche E, Shafer T J. Neural progenitor cells as models for high-throughput screens of developmental neurotoxicity: State of the science. *Neurotoxicol Teratol*, 2010, 32(1): 4-15.
- [32] Qin X Y, Akanuma H, Wei F F, Nagano R, Zeng Q, Imanishi S, Ohsako S, Yoshinaga J, Yonemoto J, Tanokura M, Sone H. Effect of low-dose thalidomide on dopaminergic neuronal differentiation of human neural progenitor cells: A combined study of metabolomics and morphological analysis. *Neurotoxicology*, 2012, 33(5): 1375-1380.
- [33] Paganoni S, Ferreira A. Neurite extension in central neurons: A novel role for the receptor tyrosine kinases *ror1* and *ror2*. *J Cell Sci*, 2005, 118(Pt 2): 433-446.
- [34] Kandasamy M, Lehner B, Kraus S, Sander P R, Marschallinger J, Rivera F J, Trumbach D, Ueberham U, Reitsamer H A, Strauss O, Bogdahn U, Couillard-Despres S, Aigner L. Tgf-beta signalling in the adult neurogenic niche promotes stem cell quiescence as well as generation of new neurons. *J Cell Mol Med*, 2014, 31(2): 5-26.
- [35] Shaker T, Dennis D, Kurrasch D M, Schuurmans C. *Neurog1* and *neurog2* coordinately regulate development of the olfactory system. *Neural development*, 2012, 7: 28-55.
- [36] Wilkinson G, Dennis D, Schuurmans C. Proneural genes in neocortical development. *Neuroscience*, 2013, 253: 256-273.
- [37] Moors M, Cline J E, Abel J, Fritsche E. Erk-dependent and -independent pathways trigger human neural progenitor cell migration. *Toxicol Appl Pharmacol*, 2007, 221(1): 57-67.
- [38] Moors M, Vudattu N K, Abel J, Kramer U, Rane L, Ulfig N, Ceccatelli S, Seyfert-Margolies V,

- Fritsche E, Maeurer M J. Interleukin-7 (il-7) and il-7 splice variants affect differentiation of human neural progenitor cells. *Genes and immunity*, 2010, 11(1): 11-20.
- [39] Halper J, Kjaer M. Basic components of connective tissues and extracellular matrix: Elastin, fibrillin, fibulins, fibrinogen, fibronectin, laminin, tenascins and thrombospondins. *Progress In Heritable Soft Connective Tissue Diseases*, 2014, 802: 31-47.
- [40] Choy M Y, St Whitley G, Manyonda I T. Efficient, rapid and reliable establishment of human trophoblast cell lines using poly-l-ornithine. *Early pregnancy*, 2000, 4(2): 124-143.
- [41] Darrabie M D, Kendall W F, Jr., Opara E C. Characteristics of poly-l-ornithine-coated alginate microcapsules. *Biomaterials*, 2005, 26(34): 6846-6852.
- [42] Ido H, Nakamura A, Kobayashi R, Ito S, Li S, Futaki S, Sekiguchi K. The requirement of the glutamic acid residue at the third position from the carboxyl termini of the laminin gamma chains in integrin binding by laminins. *J Biol Chem*, 2007, 282(15): 11144-11154.
- [43] El-Ghannam A, Starr L, Jones J. Laminin-5 coating enhances epithelial cell attachment, spreading, and hemidesmosome assembly on ti-6al-4v implant material in vitro. *J Biomed Mater Res*, 1998, 41(1): 30-40.
- [44] Kikkawa Y, Sasaki T, Nguyen M T, Nomizu M, Mitaka T, Miner J H. The lg1-3 tandem of laminin alpha 5 harbors the binding sites of lutheran/basal cell adhesion molecule and alpha 3 beta 1/alpha 6 beta 1 integrins. *J Biol Chem*, 2007, 282(20): 14853-14860.
- [45] Ekblom P, Lonai P, Talts J F. Expression and biological role of laminin-1. *Matrix biology :J Soc Biol*, 2003, 22(1): 35-47.
- [46] Bougas K, Jimbo R, Vandeweghe S, Tovar N, Baldassarri M, Alenezi A, Janal M, Coelho P G, Wennerberg A. In vivo evaluation of a novel implant coating agent: Laminin-1. *Clin Implant Dent Relat Res*, 2014, 16(5): 728-735.
- [47] Gaspard N, Vanderhaeghen P. Mechanisms of neural specification from embryonic stem cells. *Curr Opin Neurobiol*, 2010, 20(1): 37-43.
- [48] Liang X, Tang Y, Duan L, Cheng S Q, Luo L, Cao X Q, Tu B J. Adverse effect of sub-chronic exposure to benzo(a)pyrene and protective effect of butylated hydroxyanisole on learning and memory ability in male sprague-dawley rat. *J Toxicol Sci*, 2014, 39(5): 739-748.

- [49] Nie J S, Zhang H M, Zhao J, Liu H J, Niu Q. Involvement of mitochondrial pathway in benzo[a]pyrene-induced neuron apoptosis. *Hum Exp Toxicol*, 2014, 33(3): 240-250.
- [50] Hossain M M, Takashima A, Nakayama H, Doi K. 5-azacytidine induces toxicity in pc12 cells by apoptosis. *Exp Toxicol Pathol*, 1997, 49(3-4): 201-206.
- [51] Ueno M, Katayama K I, Nakayama H, Doi K. Mechanisms of 5-azacytidine (5azc)-induced toxicity in the rat foetal brain. *Int J Clin Exp Pathol*, 2002, 83(3): 139-150.
- [52] Hossain M M, Takashima A, Nakayama H, Doi K. 5-azacytidine induces toxicity in pc12 cells by apoptosis. *EXP TOXICOL PATHOL*, 1997, 49(3-4): 201-206.
- [53] Miyazaki T, Futaki S, Suemori H, Taniguchi Y, Yamada M, Kawasaki M, Hayashi M, Kumagai H, Nakatsuji N, Sekiguchi K, Kawase E. Laminin e8 fragments support efficient adhesion and expansion of dissociated human pluripotent stem cells. *Nature communications*, 2012, 3: 12-36.
- [54] Shiraki N, Yamazoe T, Qin Z, Ohgomori K, Mochitate K, Kume K, Kume S. Efficient differentiation of embryonic stem cells into hepatic cells in vitro using a feeder-free basement membrane substratum. *Plos One*, 2011, 6(8): 242-268.
- [55] Qin X Y, Akanuma H, Wei F, Nagano R, Zeng Q, Imanishi S, Ohsako S, Yoshinaga J, Yonemoto J, Tanokura M, Sone H. Effect of low-dose thalidomide on dopaminergic neuronal differentiation of human neural progenitor cells: A combined study of metabolomics and morphological analysis. *Neurotoxicology*, 2012, 33(5): 1375-1380.
- [56] Chepelev N L, Moffat I D, Bowers W J, Yauk C L. Neurotoxicity may be an overlooked consequence of benzo[a]pyrene exposure that is relevant to human health risk assessment. *Mutation research*, 2015, 764: 64-89.
- [57] Schellenberger M T, Grova N, Farinelle S, Willieme S, Schroeder H, Muller C P. Modulation of benzo[a]pyrene induced neurotoxicity in female mice actively immunized with a b[a]p-diphtheria toxoid conjugate. *Toxicol Appl Pharmacol*, 2013, 271(2): 175-183.
- [58] Ueno M, Katayama K, Nakayama H, Doi K. Mechanisms of 5-azacytidine (5azc)-induced toxicity in the rat foetal brain. *Int J Clin Exp Pathol* 2002, 83(3): 139-150.
- [59] Weisman S J, Berkow R L, Weetman R M, Baehner R L. 5-azacytidine: Acute central nervous system toxicity. *J Pediatr Hematol Oncol*, 1985, 7(1): 86-88.

- [60] Dobrovolskaia M A, Patri A K, Simak J, Hall J B, Semberova J, De Paoli Lacerda S H, Mcneil S E. Nanoparticle size and surface charge determine effects of pamam dendrimers on human platelets in vitro. *Mol Pharm*, 2012, 9(3): 382-393.
- [61] Albertazzi L, Gherardini L, Brondi M, Sulis Sato S, Bifone A, Pizzorusso T, Ratto G M, Bardi G. In vivo distribution and toxicity of pamam dendrimers in the central nervous system depend on their surface chemistry. *Mol Pharm*, 2013, 10(1): 249-260.